doi.org/10.26434/chemrxiv.12203066.v1

Adrenergic Modulation with Photochromic Ligands

Davia Prischich, Alexandre M. J. Gomila, Santiago Milla-Navarro, Gemma Sangüesa, Rebeca Diez-Alarcia, Beatrice Preda, Carlo Matera, Montserrat Batlle, Laura Ramírez, Ernest Giralt, Jordi Hernando, Eduard Guasch, J. Javier Meana, Pedro de la Villa, Pau Gorostiza

Submitted date: 27/04/2020 • Posted date: 28/04/2020

Citation information: Prischich, Davia; Gomila, Alexandre M. J.; Milla-Navarro, Santiago; Sangüesa, Gemma; Diez-Alarcia, Rebeca; Preda, Beatrice; et al. (2020): Adrenergic Modulation with Photochromic Ligands. ChemRxiv. Preprint. https://doi.org/10.26434/chemrxiv.12203066.v1

Adrenoceptors are ubiquitous and regulate heart and respiratory rate, digestion, metabolism, and vascular tone. They can be activated or blocked with adrenergic drugs, but systemic administration causes broad adverse effects. We have developed photochromic ligands (adrenoswitches) to switch on and off adrenoceptor activity on demand at selected locations. Their pharmacology, photochromism, bioavailability and lack of toxicity allow photomodulating adrenergic signalling, as demonstrated by controlling locomotion in zebrafish and pupillary responses in blind mice.

Adrenergic modulation with photochromic ligands

Davia Prischich[1,2], Alexandre M. J. Gomila[1,2], Santiago Milla-Navarro[3], Gemma Sangüesa[4,5], Rebeca Diez-Alarcia[6,7], Beatrice Preda[1], Carlo Matera[1,2], Montserrat Batlle[4,5], Laura Ramírez[3], Ernest Giralt[8,9], Jordi Hernando[10], Eduard Guasch[4,5], J. Javier Meana[6,7], Pedro de la Villa[3,11], Pau Gorostiza[1,2,12,*]

1. Institute for Bioengineering of Catalonia (IBEC), The Barcelona Institute for Science and Technology, Barcelona, Spain
2. Centro de Investigación Biomédica en Red – Bioingeniería, Biomateriales y Nanomedicina (CIBER-BBN), Madrid, Spain
3. Department of Systems Biology, University of Alcalá (UAH), Madrid, Spain
4. Institut Clínic Cardiovascular, Hospital Clinic, University of Barcelona (UB), IDIBAPS, Barcelona, Spain
5. Centro de Investigación Biomédica en Red – Enfermedades Cardiovasculares (CIBER-CV), Madrid, Spain
6. Department of Pharmacology, University of the Basque Country (UPV/EHU), Leioa, Bizkaia, Spain.
7. Centro de Investigación Biomédica en Red - Salud Mental (CIBER-SAM), Bilbao, Spain.
8. Department of Inorganic and Organic Chemistry, University of Barcelona (UB), Barcelona, Spain
9. Institute for Research in Biomedicine (IRB), Barcelona Institute for Science and Technology (BIST), Barcelona, Spain
10. Departament de Química, Universitat Autònoma de Barcelona (UAB), Cerdanyola del Vallès, Spain
11. Instituto Ramón y Cajal de Investigación Sanitaria (IRYCIS), Madrid, Spain
12. Catalan Institution for Research and Advanced Studies (ICREA), Barcelona, Spain

(*) E-mail: pau@icrea.cat

Abstract: Adrenoceptors are ubiquitous and regulate heart and respiratory rate, digestion, metabolism, and vascular tone. They can be activated or blocked with adrenergic drugs, but systemic administration causes broad adverse effects. We have developed photochromic ligands (adrenoswitches) to switch on and off adrenoceptor activity on demand at selected locations. Their pharmacology, photochromism, bioavailability and lack of toxicity allow photomodulating adrenergic signalling, as demonstrated by controlling locomotion in zebrafish and pupillary responses in blind mice.

Adrenergic neurotransmission plays an essential role over our body's unconscious regulation of vital functions such as heart and respiratory rate, digestion, smooth-muscle contraction, gland secretion and pupil diameter. More generally, it is part of that branch of the autonomic nervous system known as sympathetic nervous system (SNS), which mobilizes a rapid response whenever a situation of acute stress and/or danger is presented. Because of the almost ubiquitous innervation of the sympathetic fibres, adrenergic receptors (ARs), both α and β subtypes, are extensively expressed in the human body. Over the years, this has made them extremely attractive and fruitful targets for pharmaceutical research and industry. Adrenergic modulators are used to effectively treat a variety of conditions such as hypertension, asthma, glaucoma, rhinitis, depression, heart failure, several types of cardiac arrhythmias, anaphylaxis, and migraine. However, the list of potential side effects is even longer, which hampers the use of the aforementioned treatments or lowers their tolerability[1]. Limitations of classical pharmacotherapy are mainly ascribable to poor drug selectivity and are the most restrictive when it comes to agents characterized by low therapeutic indices (i.e. high acute toxicity) and/or by the necessity of chronic and systemic administration (i.e. protracted exposure to off-target effects, low compliance). In this regard, photopharmacology allows to precisely deliver drug activity in space and time[2,3]. Photochromic groups that respond to specific light stimulation (e.g. azobenzene, which reversibly photoisomerizes between *cis* and *trans* configurations) are introduced into the structure of bioactive compounds thus allowing for non-invasive, on-demand control over a variety of biological targets. Successful examples of photoswitchable drugs include small molecule ligands of ion channels, receptors and enzymes, peptides, lipids and nucleic acids[4]. However,

despite the expanding applications of photopharmacology, drugs to photoswitch adrenergic neurotransmission are not available. Considering the physiological importance of the sympathetic system, we aimed our efforts at developing a small library of novel adrenergic ligands that could be remotely and dynamically controlled with light. Among the large database of sympatholytic and sympathomimetic agents built over decades of investigation, we focused our attention on a class of cyclic amidines structurally related to clonidine and to other widely commercialized drugs targeting α-ARs. (**Figure 1A**).

All adrenergic agents can be simplified to a common pharmacophoric motif, which consists in a primary or secondary aliphatic amine, protonated at physiological pH, and separated by a short linker (1-3 atoms) from a substituted benzene ring. We postulated that α-adrenergic ligands were suitable candidates for "azologization"[5,6] as the structural changes required to obtain photo-responsive derivatives could be introduced without altering essential pharmacophoric elements. In addition, the prospect of obtaining dark-inactive adrenergic azologs was supported by the lack of biological activity of *trans*-like epoxydic analogues compared to *cis*-like compounds[7]. We thus designed a set of putative photoswitchable adrenergic ligands, named "adrenoswitches", by replacing the two-atom linker with an azo group while constraining the cyclic amidine moiety to the closest structurally related aromatic derivatives. Since small structural changes can drastically alter the pharmacological profile of the molecules[8–11], we opted for a classical medicinal chemistry approach maintaining unvaried the substituted benzene moiety while exploring different heterocycles in order to afford both adrenergic activity and photochromism. The *ortho*-dichlorobenzene system common to clonidine and lofexidine seemed a feature worth maintaining for both purposes. First, halogen substitution increases the lipophilicity of a molecule, thus improving its absorption and its permeability to the blood brain barrier or the blood ocular barrier[12]. This property is correlated with the potency of hypotensive agents acting on the central nervous system (CNS)[13,14]. Moreover, lipophilic substitutions at the positions 2 and 6 of the phenyl ring are well tolerated in terms of pharmacological activity both by α_1- and α_2-ARs[15]. Secondly, from a photochromic point of view, *ortho*-halogenated azobenzenes benefit of enhanced thermal stability, longer photoisomerization wavelengths, and higher isomerization ratios when compared to their parent compounds[16–18].

Having defined the hydrophobic moiety and the photoresponsive bridge of our derivatives, we moved on to identify suitable aromatic heterocycles. In our first analogue (adrenoswitch-1, **Figure 1B**) we substituted the imidazoline ring with an imidazole. As phenylazoimidazoles are known to undergo fast *cis-trans* thermal back-isomerization (i.e. fast-relaxing photoswitches), in adrenoswitch-2 we sought to reduce the rate of this process by employing an *N*-methyl imidazole[19]. In adrenoswitch-3, we introduced a permanent positive charge with a *N*,*N*-dimethyl imidazolium in order to better mimic the electronic properties of the original cyclic amidine in its physiologically protonated form. An alternative strategy for the same purpose was using 2-aminothiazole in adrenoswitch-4.

Our library of compounds was prepared via a divergent synthetic approach involving a standard azo coupling reaction (**Figure 1B**). Commercially available 2,6-dichloroaniline was converted into the corresponding diazonium salt and reacted under mild basic conditions either with imidazole to provide adrenoswitch-1 or with 2-aminothiazole to afford adrenoswitch-4. Adrenoswitch-2 and adrenoswitch-3 were obtained from adrenoswitch-1 through reactions of mono- or di-*N*-methylation, respectively.

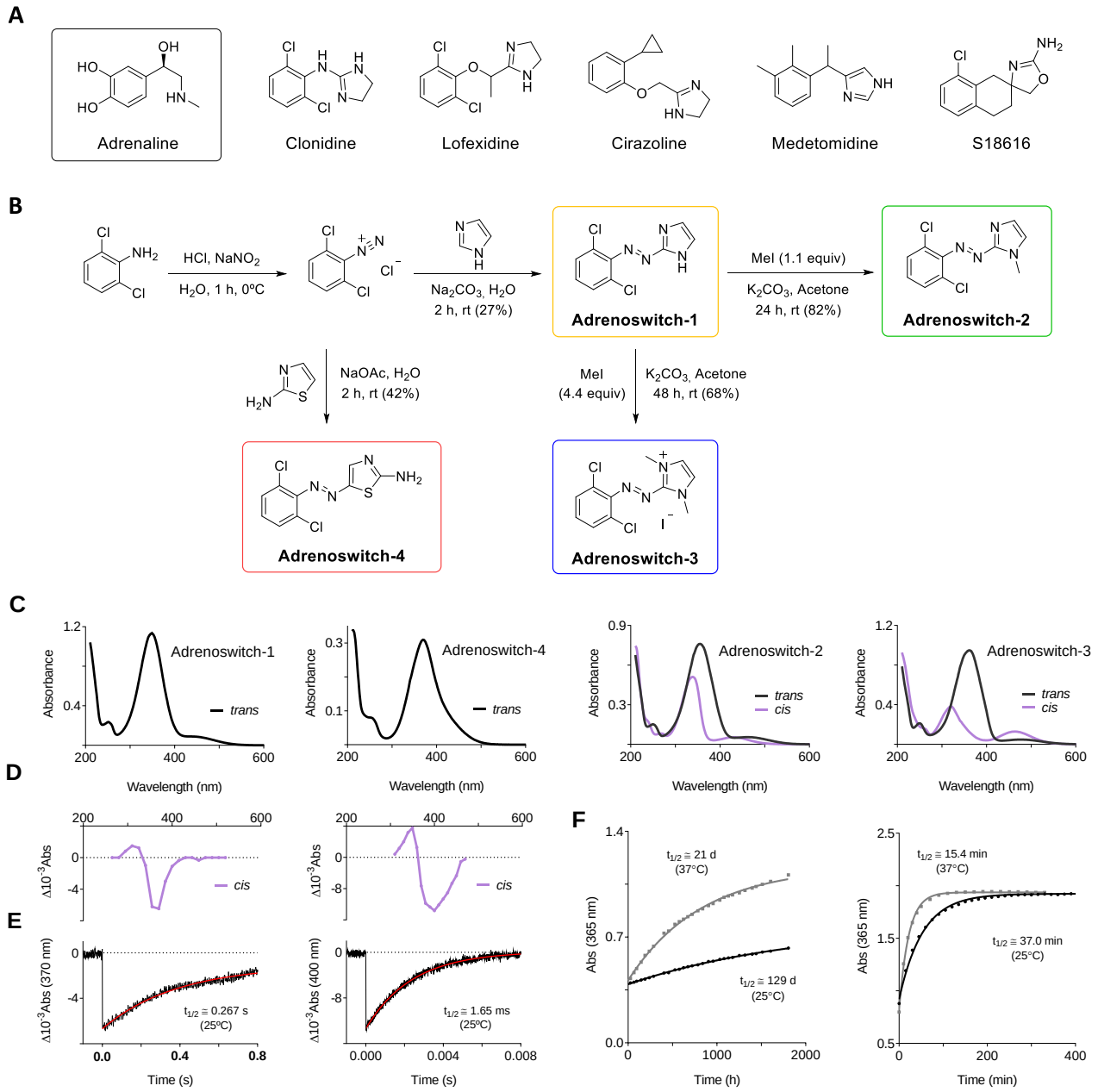

Figure 1. A) Chemical structures of adrenaline and some of the synthetic adrenergic ligands that inspired this work. **B)** Divergent chemical synthesis of adrenoswitches 1-4. **C)** UV-Vis absorption spectra of the *trans* isomers, for slow-relaxing adrenoswitches -2 and -3, UV-Vis absorption spectra of the *cis* isomers are also reported. Spectra were extracted from UPLC chromatograms after elution with a mixture of water and acetonitrile supplemented with trifluoroacetic acid. Spectra of *cis* and *trans* isomers were normalized at their isosbestic points (see SI – **Figures S3A-C**). **D)** Transient absorption spectra of adrenoswitch-1 and -4 at $t = 0$ upon pulsed excitation at $\lambda_{exc} = 355$ nm in physiological buffer (pH=7.4 at 25°C). **E)** Absorption loss and recovery kinetics of adrenoswitch-1 and adrenoswitch-4, measured at $\lambda = 370$ and 400 nm respectively, upon irradiation with a single ns laser pulse (t=0) at $\lambda_{exc} = 355$ nm and 25 °C in physiological buffer (pH=7.4). Red lines correspond to monoexponential fitting of the experimental data. **F)** *Cis*-to-*trans* thermal relaxation of adrenoswitch-2 and -3 at 25 ˚C (in black) and 37 ˚C (in gray) under dark conditions. Data were fitted to a monoexponential decay model to estimate the half-lives of the *cis* isomers.

The photochromic behaviour of our compounds was then investigated. It is worth mentioning that, although several azoheteroaryl photoswitches have been already reported in the literature[20], the photoswitches contained in our compounds have never been described before. Slow-relaxing adrenoswitch-2 and -3 were characterized by steady-state UV-Vis absorption spectroscopy (**Figures 1C-F**), while transient UV-Vis absorption spectroscopy was used for fast-relaxing adrenoswitch-1 and -4 (**Figures 1D-E**). All our compounds

can be photoisomerized from *trans* to *cis* with (ultra)violet light (365–400 nm) and from *cis* to *trans* with blue or green light (450–500 nm). As intended by design, thermal relaxation rates vary considerably along the series. Measured half-lives spanned from milliseconds (adrenoswitch-4) to seconds (adrenoswitch-1), minutes (adrenoswitch-3), and months (adrenoswitch-2) (**Figures 1E-F**).

With all the information in hand to effectively photoswitch our ligands, we moved on to assess their biological activity as a function of illumination. The affinity of the library towards α_2-ARs was measured by competitive radioligand binding assay in pre-frontal cortex membranes obtained *post mortem* from human brains. All the adrenoswitches competed in binding to the receptor albeit at weaker affinities than clonidine. Most notably, the slow-relaxing adrenoswitch-2 and -3 showed a significant change in binding potency upon UV illumination (**Figure S4A**).

Since the adrenergic system is a major regulator of the vascular tone, we further characterized the adrenergic effects of our compounds by measuring their vasoconstrictor/vasodilatory activity in *ex vivo* rat aortic rings where the endothelium had been preserved[21–25]. Compounds were first screened for their vasoconstrictor potencies by cumulative additions on plain quiescent vessels, on which they all proved unable to evoke contractions. Subsequently, we examined their vascular activity on rings pre-contracted with phenylephrine (PE). We observed that vascular smooth muscle relaxes when exposed to UV light alone, substantially abolishing the contraction evoked by PE[26]. These intrinsic photoresponses are due to nitric oxide (NO) release either from endogenous or exogenous donors or from storage vesicles[27,28]. To minimize unintended photorelaxation, we pre-incubated the vessels in a suitable nitric oxide synthase (NOS) inhibitor, namely N^G-methyl-L-arginine acetate (L-NMMA) which is reported to be unaffected by light[29]. Remarkably, all adrenoswitches displayed high vasodilatory efficacies (maximal evoked response E_{max}, **Figure 2A**) with adrenoswitch-1 coming through as the most potent compound and the only one displaying a light-dependent behavior in this assay (3x increase in potency upon UV illumination, **Figure S8A**). Although this assay was useful to identify and rank the adrenergic efficacy and potency of adrenoswitches, it had important shortcomings. Intrinsic photoresponses forced us to use a NOS inhibitor, thus partially blocking endothelium-dependent relaxation responses to α_2-AR agonists[30,31]. Moreover, the model proved complex to clarify adrenergic pharmacodynamics and it cannot exclude contribution of other receptors to the observed antihypertensive responses.

We next characterized the activity of adrenoswitches *in vivo*. Zebrafish (*Danio rerio*) is a well established animal model for neurobehavioural research[32,33] and toxicological studies,[34,35] and the transparency of their larvae makes them convenient for photopharmacological applications[36–39]. The expression and function of zebrafish ARs have been studied[40,41] and the effect of dexmedetomidine, a central-acting and structurally-related α_2-AR agonist, has also been described by Ruuskanen *et al.*[42].

In analogy to the sedative effect reported for dexmedetomidine, administration of clonidine (50 µM) caused locomotor inhibition when compared to untreated control animals (**Figure 2B**, fish trajectories shown in light blue and grey wells respectively). Clonidine effect was not significantly altered by UV illumination, although in vehicle-treated animals we observed an increase of the swimming distances as a result of their photomotor response to UV light.[33] In contrast, larvae treated with adrenoswitch-1 (50 µM) responded to UV light by progressively reducing their locomotion to levels comparable to clonidine-treated animals under UV (**Figures 2B-C and Figures S9-S10**). Therefore, adrenoswitch-1 displayed a clonidine-like behaviour upon activation with UV light, while its *trans* isomer was unable to evoke sedation. Although this effect is unequivocally light-induced, it did not revert after turning the light off despite the fast-relaxing nature of the compound (**Figure 1E and Figure S10**). Moreover, this behavioural set-up cannot exclude the involvement of other non-

adrenergic receptors in evoking locomotion responses. We thus continued studying adrenoswitch-1 in a different *in vivo* model.

Among the available experimental models for assessing autonomic responses *in vivo*, we sought one in which the adrenergic system played a major physiological role, and in which the target tissue was easily accessible to light. The quantification of mydriatic or miotic responses by pupillometry fulfilled both criteria.[43] In addition, this assay allows for a selective evaluation of α-adrenergic activity and it excludes the involvement of other targets, most notably imidazoline receptors[44–46]. As pupils naturally adapt their diameter in response to changes in light intensity (pupillary light reflex), we resorted to genetically engineered mice (*Opn4xRd10*). These animals do not express melanopsin and their rods and cones degenerate two months after their birth, thus becoming physiologically insensitive to any luminous stimuli. We tested if adrenoswitch-1 enabled photoregulation of pupil diameter after topical administration (1 mM, 0.02% w/v) to isoflurane-anesthetized blind mice. We observed that the compound exerted mydriasis only under concomitant UV illumination, and that the effects were reversed in the absence of light, which causes adrenoswitch-1 to rapidly relax to the *trans* configuration (**Figures 2D-E-F**). These pupillary responses were reproducible in at least two cycles of alternating UV light and darkness, and were neither elicited by application of the vehicle nor by exposure to UV light alone. The maximum photoresponses were consistently observed after approximately 20 min from its administration (**Figure 2F**), in agreement with the pharmacodynamics of adrenergic ligands with similar structure and lipophilicity to adrenoswitch-1[47].

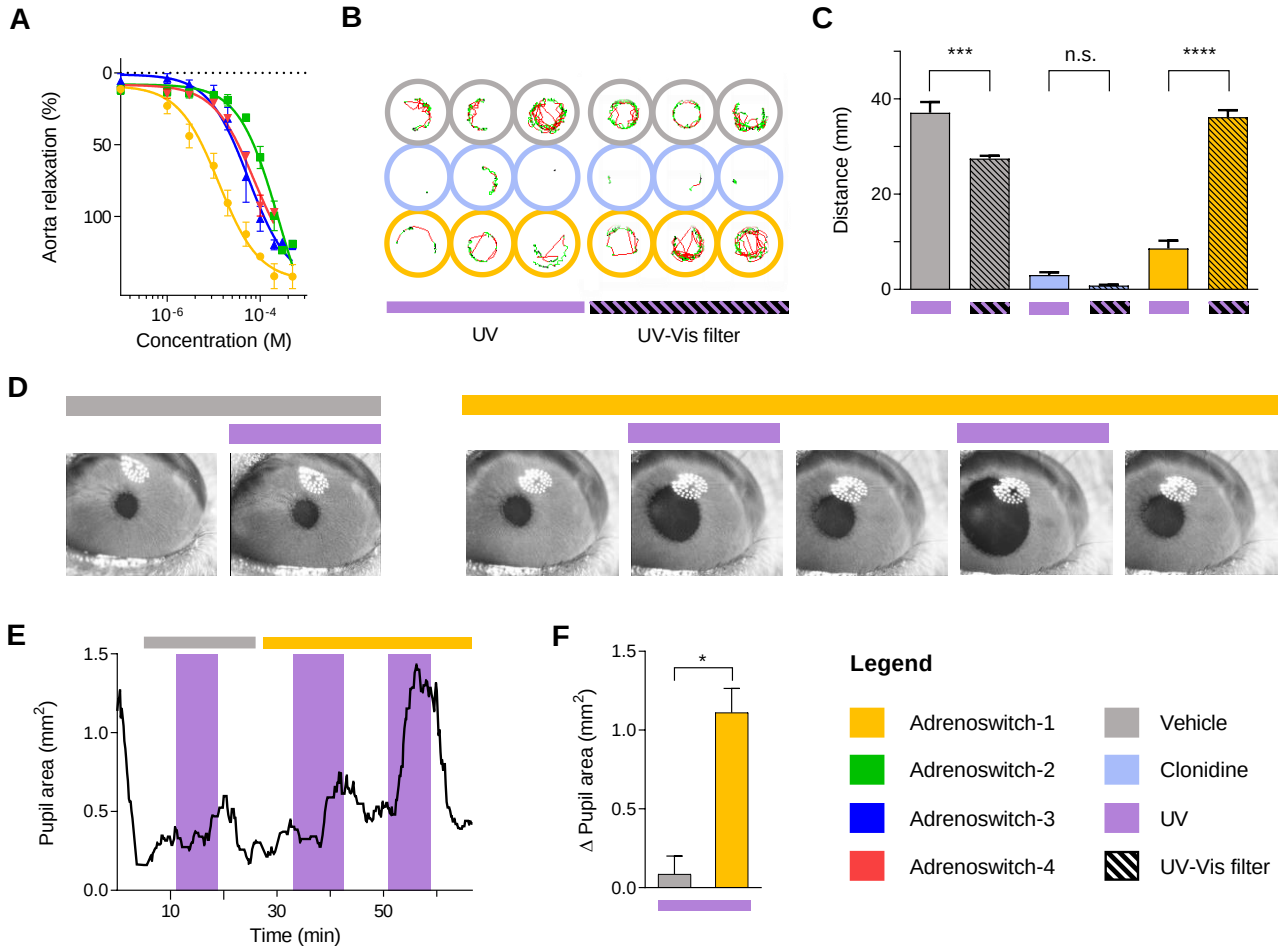

Figure 2. A) Dose-response curves comparing the vasodilatory potencies of *cis*-enriched adrenoswitches administered under UV illumination to rat aortic rings where the endothelium had been preserved. Vessels were pre-contracted with 10^{-6} M phenylephrine after treatment with 10^{-3} M N^{G}-methyl-L-arginine acetate (L-NMMA), a nitric oxide synthase inhibitor. Relaxation is expressed as

percentages of the reference contraction induced by PE. Data are means ± SEM (adrenoswitches 1-3, *n*=4; adrenoswitch-4, *n*=2). **B)** *Danio rerio* 7 days post-fertilisation (dpf) larvae swimming trajectories (movements with velocities over 6 mm·s^{-1}) after treatment with the vehicle (grey wells), 50 µM clonidine (light-blue wells) and 50 µM adrenoswitch-1 (yellow wells). Conditions were simultaneously analysed under 365 nm UV illumination (left panel, *cis*-enriched adrenoswitch-1) and under a UV-Vis filter (right panel, *trans* adrenoswitch-1) that only transmit infrared light for movement recording. **C)** Quantification of the swimming trajectories shown in **B)** after 20 minutes in the presence of the vehicle (grey), 50 µM clonidine (light blue) and 50 µM adrenoswitch-1 (yellow) under UV illumination or under a UV -Vis filter (shades bars). Data are means ± SEM (*n*=12 per treatment). Statistical differences between UV- and non-UV-exposed larvae were determined by two-way ANOVA with Tukey's multiple comparison test (n.s., not significant; ***, *p*-value<0.01; ****, *p*-value<0.001) **D-E)** Pupillary responses in an isoflurane-anestethized *Opn4xRd10* blind mouse first treated with the vehicle and then administered 1 mM adrenoswitch-1 in its right eye. Adrenoswitch-1 exerted mydriasis only under concomitant UV illumination. Nor the vehicle nor UV light alone elicited any pupillary responses in the animals. **F)** Change in area of vehicle vs. adrenoswitch-1 treated pupils of *Opn4xRd10* blind mice at 20 minutes from administration of the drug when under concomitant UV illumination. Data are means ± SEM (*n*=4 per condition). Statistical differences were determined determined by Student's *t* test for paired observations.

As mydriasis is mediated by postsynaptic α-adrenoceptors of the iris smooth muscle dilator, the results of **Figures 2D-E-F** unambiguously demonstrate that adrenoswich-1 modulates endogenous ARs with light. This opens the way to multiple applications in the SNS and CNS that were not previously accessible. For example on-demand adrenergic modulation at specific locations might allow to blunt hypertension, to treat glaucoma, or to single out individual adrenergic projections from the locus coeruleus. In addition to these novel applications, spatiotemporal modulation of adrenoceptors should improve the efficacy of treatments (including higher doses) and prevent side effects.

Optogenetic control of adrenoceptors has been shown but it requires overexpressing opsins in the target tissue using genetic manipulation, and thus several safety and regulatory hurdles should be overcome for therapeutic purposes[48–51]. Currently the only way to target endogenous receptors and physiological adrenergic pathways is by means of drugs. Uncaging of adrenergic ligands is irreversible and releases undesired by-products[52,53]. Here, we have rationally designed novel arylazoheteroarene reversible photoswitches and characterised their adrenergic action *in vitro* and *in vivo*. The drug-like properties of these adrenoswitches, the absence of acute toxicity in zebrafish larvae and most remarkably, the fact that adrenergic (photo)modulation was readily and reversibly achieved in mammals by topical application without formulation, all indicate that adrenergic photomodulation offers unique opportunities to understand physiological signaling and to develop safe and effective therapies.

Acknowledgements:
Mass spectrometry was performed at the IRB Barcelona Mass Spectrometry Core Facility, which actively participates in the BMBS European COST Action BM 1403 and is a member of Proteored, PRB2-ISCIII, supported by grant PRB2 (IPT13/0001 − ISCIIISGEFI/FEDER). This research received funding from the European Union Research and Innovation Programme Horizon 2020 (Human Brain Project SGA2 Grant Agreement 785907, WaveScalES), European Research ERA-Net SynBio programme (Modulightor project), Agency for Management of University and Research Grants/Generalitat de Catalunya (CERCA Programme; 2017-SGR-1442 and 2017-SGR-00465 projects; RIS3CAT plan), Fonds Européen de Développement Économique et Régional (FEDER) funds, Ministry of Economy and Competitiveness (Grant CTQ2016-80066-R), Institute of Health Carlos III (IP18/00754), Fundaluce and "la Caixa" foundations (ID 100010434, agreement LCF/PR/HR19/52160010) and Basque Government (IT-1211-19). D.P. was supported by fellowship BES-2015-072657. A.M.J.G. was supported by fellowship BES-2015-072657.

1. Farzam, K. & Lakhkar, A. *Adrenergic Drugs*. (StatPearls Publishing, 2019).

2. Velema, W. A., Szymanski, W. & Feringa, B. L. Photopharmacology: Beyond proof of principle. *J. Am. Chem. Soc.* **136**, 2178–2191 (2014).

3. Hüll, K., Morstein, J. & Trauner, D. In Vivo Photopharmacology. *Chem. Rev.* **118**, 10710–10747 (2018).

4. Lerch, M. M., Hansen, M. J., van Dam, G. M., Szymanski, W. & Feringa, B. L. Emerging Targets in Photopharmacology. *Angew. Chemie - Int. Ed.* **55**, 10978–10999 (2016).

5. Pittolo, S. *et al.* An allosteric modulator to control endogenous G protein-coupled receptors with light. *Nat. Chem. Biol.* **10**, 813–815 (2014).

6. Schoenberger, M., Damijonaitis, A., Zhang, Z., Nagel, D. & Trauner, D. Development of a new photochromic ion channel blocker via azologization of fomocaine. *ACS Chem. Neurosci.* **5**, 514–518 (2014).

7. Gentili, F. *et al.* α2-adrenoreceptors profile modulation. 2.1 Biphenyline analogues as tools for selective activation of the α2C-subtype. *J. Med. Chem.* **47**, 6160–6173 (2004).

8. Rodriguez, F., Rozas, I., Ortega, J. E., Meana, J. J. & Callado, L. F. Guanidine and 2-aminoimidazoline aromatic derivatives as α2-adrenoceptor antagonists, 1: Toward new antidepressants with heteroatomic linkers. *J. Med. Chem.* **50**, 4516–4527 (2007).

9. Rodriguez, F. *et al.* Guanidine and 2-aminoimidazoline aromatic derivatives as α2-adrenoceptor antagonists. 2. Exploring alkyl linkers for new antidepressants. *J. Med. Chem.* **51**, 3304–3312 (2008).

10. Rodriguez, F. *et al.* Guanidine and 2-aminoimidazoline aromatic derivatives as α2-adrenoceptor ligands: Searching for structure - activity relationships. *J. Med. Chem.* **52**, 601–609 (2009).

11. Saczewski, J. *et al.* Transfer of SAR information from hypotensive indazole to indole derivatives acting at α-adrenergic receptors: In vitro and in vivo studies. *Eur. J. Med. Chem.* **115**, 406–415 (2016).

12. Meanwell, N. A. Synopsis of some recent tactical application of bioisosteres in drug design. *J. Med. Chem.* **54**, 2529–2591 (2011).

13. Timmermans, P. B. M. W. M., Brands, A. & van Zwieten, P. A. Lipophilicity and brain disposition of clonidine and structurally related imidazolidines. *Naunyn. Schmiedebergs. Arch. Pharmacol.* **300**, 217–226 (1977).

14. Nasal, A., Fr, T., Petrusewicz, J., Bucifiski, A. & Kaliszan, R. Mydriasis elicited by imidazol(in)e α2-adrenomimetics in comparison with other adrenoceptor-mediated effects and hydrophobicity. **274**, 125–132 (1995).

15. Nichols, A. J. & Ruffolo, R. R. Structure-Activity Relationships for α-Adrenoceptor Agonists and Antagonists. in *Alpha-Adrenoceptors: Molecular Biology, Biochemistry and Pharmacology* vol. 8 75–114 (1991).

16. Bléger, D., Schwarz, J., Brouwer, A. M. & Hecht, S. O -fluoroazobenzenes as readily synthesized photoswitches offering nearly quantitative two-way isomerization with visible light. *J. Am. Chem. Soc.* **134**, 20597–20600 (2012).

17. Knie, C. *et al.* Ortho-Fluoroazobenzenes: Visible Light Switches with Very Long-Lived Z Isomers. *Chem. - A Eur. J.* **20**, 16492–16501 (2014).

18. Calbo, J., Thawani, A. R., Gibson, R. S. L., White, A. J. P. & Fuchter, M. J. A combinatorial approach to improving the performance of azoarene photoswitches. *Beilstein J. Org. Chem.* **15**, 2753–2764 (2019).

19. Otsuki, J. *et al.* Photochromism of 2-(phenylazo)imidazoles. *J. Phys. Chem. A* **109**, 8064–8069 (2005).

20. Crespi, S., Simeth, N. A. & König, B. Heteroaryl azo dyes as molecular photoswitches. *Nat. Rev. Chem.* **3**, 133–146 (2019).

21. Silva, E. G., Feres, T., Vianna, L. M., Okuyama, P. & Paiva, T. B. Dual effect of clonidine on mesenteric artery adrenoceptors: Agonistic (Alpha-2) and antagonistic (Alpha-1). *J. Pharmacol. Exp. Ther.* **277**, 872–876 (1996).

22. Wong, E. S. W., Man, R. Y. K., Vanhoutte, P. M. & Ng, K. F. J. Dexmedetomidine induces both relaxations and contractions, via different α2-adrenoceptor subtypes, in the isolated mesenteric artery and aorta of the rat. *J. Pharmacol. Exp. Ther.* **335**, 659–664 (2010).

23. Byon, H. J. *et al.* Dexmedetomidine inhibits phenylephrine-induced contractions via alpha-1 adrenoceptor blockade and nitric oxide release in isolated rat aortae. *Int. J. Med. Sci.* **14**, 143–149 (2017).

24. Ruffolo, R. R. & Waddell, J. E. Receptor interactions of imidazolines. IX. Cirazoline is an alpha-1 adrenergic agonist and an alpha-2 adrenergic antagonist. *J. Pharmacol. Exp. Ther.* **222**, 29–36 (1982).

25. Agrawal, D. K., Triggle, C. R. & Daniel, E. E. Pharmacological characterization of the postsynaptic alpha adrenoceptors in vascular smooth muscle from canine and rat mesenteric vascular beds. *J. Pharmacol. Exp. Ther.* **229**, 831–838 (1984).

26. Furchgott, R. F., Ehrreich, S. J. & Greenblatt, E. The photoactivated relaxation of smooth muscle of rabbit aorta. *J. Gen. Physiol.* **44**, 499–519 (1961).

27. Andrews, K. L., McGuire, J. J. & Triggle, C. R. A photosensitive vascular smooth muscle store of nitric oxide in mouse aorta: No dependence on expression of endothelial nitric oxide synthase. *Br. J. Pharmacol.* **138**, 932–940 (2003).

28. Flitney, F. W. & Megson, I. L. Nitric oxide and the mechanism of rat vascular smooth muscle photorelaxation. *J. Physiol.* **550**, 819–828 (2003).

29. Hsp, T., Rev, C., Mol, B. & York, N. 30 . 0. 29–31 (2007).

30. Molin, J. C. & Bendhack, L. M. Clonidine induces rat aorta relaxation by nitric oxide-dependent and -independent mechanisms. *Vascul. Pharmacol.* **42**, 1–6 (2004).

31. Vanhoutte, P. M. Endothelial adrenoceptors. *J. Cardiovasc. Pharmacol.* **38**, 796–808 (2001).

32. Basnet, R. M., Zizioli, D., Taweedet, S., Finazzi, D. & Memo, M. Zebrafish larvae as a behavioral model in neuropharmacology. *Biomedicines* **7**, (2019).

33. Kokel, D. *et al.* Rapid behavior-based identification of neuroactive small molecules in the zebrafish. *Nat Chem Biol* **6**, 231–237 (2010).

34. Rubinstein, A. L. Zebrafish assays for drug toxicity screening. *Expert Opin. Drug Metab. Toxicol.* **2**, 231–240 (2006).

35. Caballero, M. V. & Candiracci, M. Zebrafish as Toxicological model for screening and recapitulate human diseases. *J. Unexplored Med. Data* **3**, 4 (2018).

36. Rovira, X. *et al.* OptoGluNAM4.1, a Photoswitchable Allosteric Antagonist for Real-Time Control of mGlu4 Receptor Activity. *Cell Chem. Biol.* **23**, 929–934 (2016).

37. Gómez-Santacana, X. *et al.* Illuminating Phenylazopyridines to Photoswitch Metabotropic Glutamate Receptors: From the Flask to the Animals. *ACS Cent. Sci.* **3**, 81–91 (2017).

38. Matera, C. *et al.* Photoswitchable Antimetabolite for Targeted Photoactivated Chemotherapy. *J. Am. Chem. Soc.* **140**, 15764–15773 (2018).

39. Afonin, S. *et al.* Light-controllable dithienylethene-modified cyclic peptides: photoswitching the in vivo toxicity in zebrafish embryos. *Beilstein J. Org. Chem.* **16**, 39–49 (2020).

40. Ruuskanen, J. O. *et al.* Conserved structural, pharmacological and functional properties among the three human and five zebrafish α 2-adrenoceptors. *Br. J. Pharmacol.* **144**, 165–177 (2005).

41. Wang, Z. *et al.* Zebrafish β-adrenergic receptor mRNA expression and control of pigmentation. *Gene*

446, 18–27 (2009).

42. Ruuskanen, J. O., Peitsaro, N., Kaslin, J. V. M., Panula, P. & Scheinin, M. Expression and function of α2-adrenoceptors in zebrafish: Drug effects, mRNA and receptor distributions. *J. Neurochem.* **94**, 1559–1569 (2005).

43. McAuliffe-Curtin, D. & Buckley, C. Review of alpha adrenoceptor function in the eye. *Eye* **3**, 472–476 (1989).

44. Raczak-Gutknecht, J., Frackowiak, T., Nasal, A. & Kaliszan, R. Mydriasis model in rats as a simple system to evaluate a2-Adrenergic activity of the imidazol(in)e compounds. *Pharmacol. Reports* **65**, 305–312 (2013).

45. Yu, Y. & Koss, M. C. Rat clonidine mydriasis model: Imidazoline receptors are not involved. *Auton. Neurosci. Basic Clin.* **117**, 17–24 (2005).

46. Ishikawa, H., Miller, D. D. & Patil, N. Comparison of post-junctional α-adrenoceptors in iris dilator muscle of humans, and albino and pigmented rabbits. *Naunyn. Schmiedebergs. Arch. Pharmacol.* **354**, 765–772 (1996).

47. Innemee, H. C. A., de Jonge, A., van Meel, J. C. A., Timmermans, P. B. M. W. M. & van Zwieten, P. A. The Effect of Selective alpha1- and alpha2-Adrenoceptor Stimulation on Intraocular Pressure in the Conscious Rabbit. *NaunynSchmiedebergs Arch. Pharmacol.* **316**, 294–298 (1981).

48. Kim, J. M. *et al.* Light-driven activation of β2-adrenergic receptor signaling by a chimeric rhodopsin containing the β2-adrenergic receptor cytoplasmic loops. *Biochemistry* **44**, 2284–2292 (2005).

49. Makowka, P. *et al.* Optogenetic stimulation of G s -signaling in the heart with high spatio-temporal precision. *Nat. Commun.* **10**, 1281 (2019).

50. Burke, P. G. R. *et al.* Optogenetic stimulation of adrenergic C1 neurons causes sleep state-dependent cardiorespiratory stimulation and arousal with sighs in rats. *Am. J. Respir. Crit. Care Med.* **190**, 1301–1310 (2014).

51. Siuda, E. R. *et al.* Optodynamic simulation of β-adrenergic receptor signalling. *Nat. Commun.* **6**, 8480 (2015).

52. Muralidharan, S., Maher, G. M., Boyle, W. A. & Nerbonne, J. M. 'Caged' phenylephrine: Development and application to probe the mechanism of α-receptor-mediated vasoconstriction. *Proc. Natl. Acad. Sci. U. S. A.* **90**, 5199–5203 (1993).

53. Muralidharan, S. & Nerbonne, J. M. Photolabile 'caged' adrenergic receptor agonists and related model compounds. *J. Photochem. Photobiol. B Biol.* **27**, 123–137 (1995).

SUPPORTING INFORMATION (SI)

Adrenergic modulation with photochromic ligands

Davia Prischich, Alexandre Gomila, Santiago Milla-Navarro, Gemma Sangüesa, Rebeca Diez-Alarcia, Beatrice Preda, Carlo Matera, Montserrat Batlle, Laura Ramírez, Ernest Giralt, Jordi Hernando, Eduard Guasch, J. Javier Meana, Pedro de la Villa, Pau Gorostiza

Contents

Chemical synthesis and analytical characterization

Abbreviations

ACN: acetonitrile; conc.: concentrated; DCM: dichloromethane; DMSO: dimethylsulfoxide; equiv: equivalent; EtOAc: ethyl acetate; EtOH: ethanol; FA: formic acid; MeOH: methanol; mQ: milliQ; NaOAc: sodium acetate; TFA: trifluoroacetic acid; rt: room temperature; *R*t: retention time.

Materials and methods

All reagents and solvents were purchased from commercial suppliers and were used without any further purification. Analytical thin layer chromatography (TLC) was performed on silica gel 60 F254 aluminium foils (Merck Millipore, Darmstadt, DE) to monitor reactions over time. Spots were visualized under 254 or 365 nm UV light and/or by using the appropriate TLC stain. Flash chromatography was performed on silica gel 60 (40-63 µm) as stationary phase (PanReac AppliChem, Darmstadt, DE); the mobile phase being a mixture of DCM/MeOH with the corresponding percentages specified for each compound.

NMR spectroscopy

Samples for nuclear magnetic resonance (NMR) were dissolved in DMSO-d_6, Methylene chloride-d_2, Methanol-d_4 or Chloroform-*d*. Spectra were recorded with a Varian Mercury 400 MHz instrument (400 MHz for ^{1}H-NMR and 101 MHz for ^{13}C-NMR) and referenced to tetramethylsilane and/or residual solvent peaks (DMSO-d_6: ^{1}H 2.50 ppm, ^{13}C 39.52 ppm; Methanol-d_4: ^{1}H 3.31 ppm, ^{13}C 49.00 ppm; Methylene chloride-d_2: ^{1}H 5.32 ppm, ^{13}C 54.00 ppm; Chloroform-*d*: ^{1}H 7.26 ppm, ^{13}C 77.16 ppm). Chemical shifts (δ) are expressed as parts-per-million (ppm) and they refer to the *trans* isomers unless differently stated. Coupling constants (J) are measured in hertz (Hz).

Chromatography

HPLC

High pressure liquid chromatography (HPLC) was performed on a Waters Alliance e2695 Separations Module equipped with an automatic injector and a Waters 2998 UV/Vis Photodiode Array Detector (Waters, Milford, MA). Samples were solved in UPLC-grade MeOH and filtered through a 0.22 µm filter before being injected on a SunFire® C18 column (100 Å, 5 µm, 150 x 4.6 mm). The mobile phase was a mixture of mQ H_2O and ACN respectively supplemented with 0.045% and 0.036% TFA (v/v). Analysis were carried out at rt applying a 0 to 100% 8-min linear gradient while keeping the flow rate at 1 ml/min. Data were acquired using the Empower™ 3 software.

UPLC and UPLC-MS

Ultra-high pressure liquid chromatography (UPLC) and UPLC coupled to mass spectrometry (UPLC-MS) were performed with an ACQUITY UPLC H-Class System (Waters, Milford, MA) equipped with a Flow Through Needle-Sample Manager (SM-FTN), column heater, quaternary solvent manager and an ACQUITY UPLC Photodiode Array (PDA) eλ Detector. UPLC-MS mass spectra were obtained with a SQ Detector2 (Waters) equipped with an electrospray ionization (ESI) interface. Empower™ 3 and MassLynx™ 4.1 were respectively used as softwares for data acquisition. Analysis were run on an ACQUITY BEH C18 (130 Å, 1.7 µm, 50 x 2 mm) column, which was

maintained at 40˚C. The mobile phase was a mixture of mQ H_2O and ACN respectively supplemented with either 0.045% and 0.036% TFA (v/v) for UPLC analysis or 0.1% and 0.07% FA (v/v) for UPLC-MS. The flow rate was maintained at 0.6 ml/min while applying 2-min long linear gradients. Samples were prepared by dissolving the solid in UPLC-grade MeOH and then filtered through a 0.22 µm filter before injection.

Mass spectroscopy

High resolution mass spectrometry (HRMS) was performed at the IRB Barcelona Mass Spectrometry and Proteomics Core Facility using either an LTQ-FT Ultra Mass Spectrometer (Thermo Scientific, Waltham, USA) or an Orbitrap Fusion Lumos (Thermo Scientific). Both spectrometers used positive Nano-Electrospray Ionization (NanoESI) with an automated nanoelectrospray for direct infusion. The compounds (1 mg) were dissolved in 100 µL of MeOH and diluted 1:100 with ACN/H_2O/FA (50:50:1) for MS analysis. The NanoMate (Advion BioSciences, Ithaca, USA) aspirated the samples from a Protein LoBind 384-well plate using disposable, conductive pipette tips. The samples were infused through the NanoESI Chip (400 nozzles in a 20x20 array) towards the mass spectrometer. Spray voltage was 1.70 kV and delivery pressure was 0.50 psi. Data were acquired with Xcalibur software, vs.2.0SR2 (Thermo Scientific). Elemental composition from experimental exact mass monoisotopic values and isotopic distributions were obtained with a dedicated algorithm integrated in the Xcalibur software. Data are reported as mass-to-charge ratio (*m*/*z*) of the corresponding positively charged molecular ions.

Synthetic procedures

Our small library of compounds was prepared using a divergent synthetic approach (**Scheme S1**). Adrenoswitch-1 and adrenoswitch-4 were synthesized from a common and commercially available precursor via a standard azo coupling reaction. The diazonium salt of 2,6-dichloroaniline was reacted under mild basic conditions either with imidazole to provide adrenoswitch-1 or with 2-aminothiazole to afford adrenoswitch-4. Reaction conditions were adapted from previously reported procedures[1,2]. Adrenoswitch-2 and adrenoswitch-3 were obtained from adrenoswitch-1 through reactions of mono- or di-*N*- methylation, respectively.

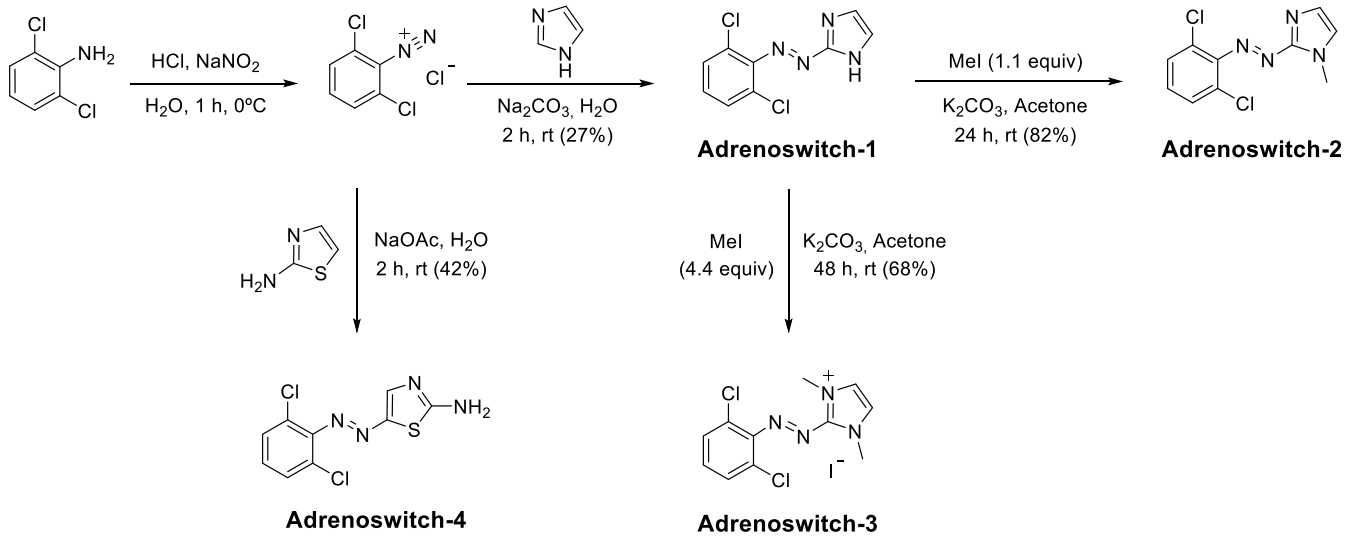

Scheme S1. Divergent synthetic route to prepare adrenoswitches 1-4.

Adrenoswitch-1

2-((2,6-dichlorophenyl)diazenyl)-1*H*-imidazole

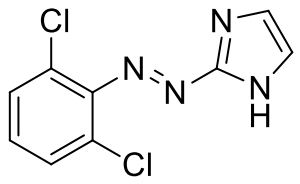

To a stirred suspension of 2,6-dichloroaniline (1.43 g, 8.83 mmol, 1.2 equiv) in mQ H_20 (32 ml) at 0˚ C was added conc. HCl (0.904 ml, 11.0 mmol, 1.5 equiv). A solution of $NaNO_2$ (709.4 mg, 10.3 mmol, 1.4 equiv) in mQ H_2O (6.4 ml) was cooled in an ice bath before being added dropwise to the mixture over an hour. Simultaneously, imidazole (500.0 mg, 7.34 mmol, 1.0 equiv) and Na_2CO_3 (1.95 g, 18.40 mmol, 2.5 equiv) were dissolved in 32 ml mQ H_2O. The solution of diazotized dichloroaniline was then slowly dripped to this mixture immediately resulting in precipitation of the crude product. The reaction was allowed to stand for 2 hours and then filtered over a P5 sintered glass filter. The precipitate was washed with cold mQ H_2O, recrystallized from a mixture of toluene and ethanol (4:1), and dried under high vacuum to give the desired compound as an orange powder (498.0 mg, 27% yield).

UPLC purity: ≥ 95% (**Figure S2.1**)

*R*t (HPLC): 5.61 min (*trans* isomer)

^{1}H NMR (400 MHz, DMSO-d_6) δ 13.39 (s, 1H), 7.64 (d, *J* = 8.2 Hz, 2H), 7.46 (s, 2H), 7.41 (dd, *J* = 8.5, 7.8 Hz, 1H). (**Figure S1.1**)

^{13}C NMR (101 MHz, DMSO-d_6) δ 155.18, 147.64, 147.64, 129.42, 129.36, 125.71. (**Figure S1.1**)

HRMS (ESI): *m/z* calculated for $C_9H_7N_4Cl_2^+$ $[M+H]^+$: 241.00423; found: 241.00272.

Adrenoswitch-2

2-((2,6-dichlorophenyl)diazenyl)-1-methyl-1*H*-imidazole

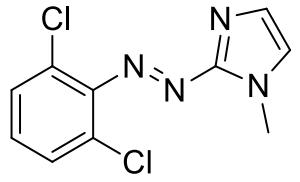

To a solution of adrenoswitch-1 (261.0 mg – 1.08 mmol) in acetone (20 ml) at rt was added solid K_2CO_3 (179.5 mg – 1.30 mmol – 1.2 equiv) and stirred for 10 minutes. 1.2 M methyl iodide in acetone (169.0 mg – 1.19 mmol – 1.1 equiv in 1.0 ml acetone) was then added dropwise to the suspension and the reaction mixture was stirred overnight at rt. The following morning all the starting material had disappered by TLC. The solvent was removed under reduced pressure and the crude was split between DCM (20 ml) and mQ H_2O (20 ml). The phases were

separated and the aqueous layer was extracted with DCM (3 × 20 ml). The organic layers were combined, dried over anhydrous $MgSO_4$, filtered and the solvent removed *in vacuo*. The crude was purified by flash chromatography through isocratic elution of DCM supplemented with 1% MeOH. Fractions containing the *trans* and *cis* isomers were combined and the solvent evaporated to afford the titled compound as an orange solid ([*trans* + *cis*]: 226.0 mg, 82% yield).

UPLC purity: ≥ 95% (**Figure S2.1**)

*R*t (HPLC): 5.58 min (*trans* isomer)

^{1}H NMR (400 MHz, Methylene chloride-d_2) δ 7.45 (d, *J* = 8.2 Hz, d, *J* = 7.9 Hz, 2H), 7.34 (d, *J* = 0.9 Hz, 1H), 7.26 (d, *J* = 0.7 Hz, 1H), 7.23 (dd, *J* = 8.5, 7.7 Hz, 1H), 4.00 (s, 3H). (*trans* isomer) (**Figure S1.2**)

^{1}H NMR (400 MHz, Methylene chloride-d_2) δ 7.32 (d, *J* = 8.4 Hz, d, *J* = 7.9 Hz, 2H), 7.13 (dd, *J* = 8.5, 7.6 Hz, 1H), 7.10 (d, *J* = 0.7 Hz, 1H), 7.02 (d, *J* = 1.0 Hz, 1H), 4.15 (s, 3H). (*cis* isomer) (**Figure S1.2**)

^{13}C NMR (101 MHz, DMSO-d_6) δ 148.70, 131.81, 129.90, 129.42, 128.15, 126.03, 33.89. (*trans* isomer) (**Figure S1.3**)

^{13}C NMR (101 MHz, DMSO-d_6) δ 152.95, 130.82, 128.71, 127.21, 124.75, 122.69, 33.72. (*cis* isomer) (**Figure S1.3**)

HRMS (ESI): *m/z* calculated for $C_{10}H_9N_4Cl_2^+$ $[M+H]^+$: 255.01988; found: 255.02014.

Adrenoswitch-3

2-((2,6-dichlorophenyl)diazenyl)-1,3-dimethyl-1*H*-imidazol-3-ium iodide

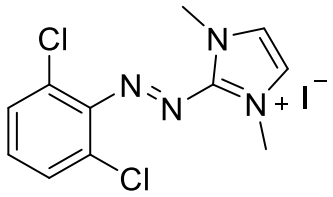

To a solution of adrenoswitch-1 (500.0 mg – 2.07 mmol) in acetone (30 ml) at rt was added solid K_2CO_3 (344.0 mg – 2.49 mmol – 1.2 equiv) and stirred for 10 minutes. A solution of 2.4 M methyl iodide in acetone (1.30 g – 9.13 mmol – 4.4 equiv in 3.8 ml acetone) was then added dropwise to the suspension. The reaction mixture was stirred at rt for 48 hours before removing the solvent under reduced pressure. The solid was resuspended in mQ H_2O (30 ml) and the aqueous phase extracted with DCM (3 × 30 ml). The organic layers were combined, dried over anhydrous $MgSO_4$, filtered and the solvent removed *in vacuo*. The crude was washed with hot EtOAc and the product finally recrystallised from EtOH to yield the desired product as burgundy needles (380.0 mg, 68% yield).

UPLC purity: ≥ 95% (**Figure S2.1**)

*R*t (HPLC): 4.80 min (*trans* isomer)

^{1}H NMR (400 MHz, Methanol-d_4) δ 7.98 (s, 2H), 7.71 (d, *J* = 8.7 Hz, d, *J* = 7.6 Hz, 2H), 7.57 (dd, *J* = 8.7, 7.5 Hz, 1H), 4.22 (s, 6H). (**Figure S1.5**)

^{13}C NMR (101 MHz, Methanol-d_4) δ 134.81, 131.89, 131.73, 127.01, 38.03. (**Figure S1.5**)

HRMS (ESI): *m/z* calculated for $C_{11}H_{11}N_4Cl_2^+$ $[M]^+$: 269.03553; found: 269.03516.

Adrenoswitch-4

5-((2,6-dichlorophenyl)diazenyl)thiazol-2-amine

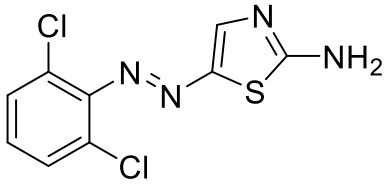

To a stirred suspension of 2,6-dichloroaniline (194 mg, 1.2 mmol, 1.2 equiv) in mQ H_20 (5.0 ml) at 0˚C was added conc. HCl (0.123 ml, 1.5 mmol, 1.5 equiv). A solution of $NaNO_2$ (96.5 mg, 1.4 mmol, 1.4 equiv) in mQ H_2O (1.0 ml) was cooled on ice and then added dropwise to the mixture over an hour. Simultaneously, 2-aminothiazole (100.0 mg, 0.99 mmol, 1.0 equiv) and NaOAc (245.7 mg, 3.0 mmol, 3.0 equiv) were dissolved in 5 ml mQ H_2O. The solution of diazotized dichloroaniline was then slowly dripped to this mixture immediately resulting in precipitation of the product. The reaction was allowed to stand for 2 hours and then filtered over a P5 sintered glass filter. The precipitate was washed with cold mQ H_2O and dried under high vacuum to give the titled product as an orange-brown powder (116.0 mg, 42% yield).

UPLC purity: $\geq$ 95% (**Figure S2.2**)

*R*t (HPLC): 7.02 min (*trans* isomer)

^{1}H NMR (400 MHz, Chloroform-*d*) δ 8.04 (s, 1H), 7.37 (d, *J* = 8.1 Hz, 2H), 7.13 (t, *J* = 8.2 Hz, 1H), 5.86 (s, 2H). (**Figure S1.6**)

^{13}C NMR (101 MHz, Chloroform-*d*) δ 171.45, 149.02, 147.38, 146.58, 129.16, 128.12, 127.93. (**Figure S1.6**)

HRMS (ESI): *m/z* calculated for $C_9H_7N_4Cl_2S^+$ $[M+H]^+$: 272.97630; found: 272.97667.

Analytical data

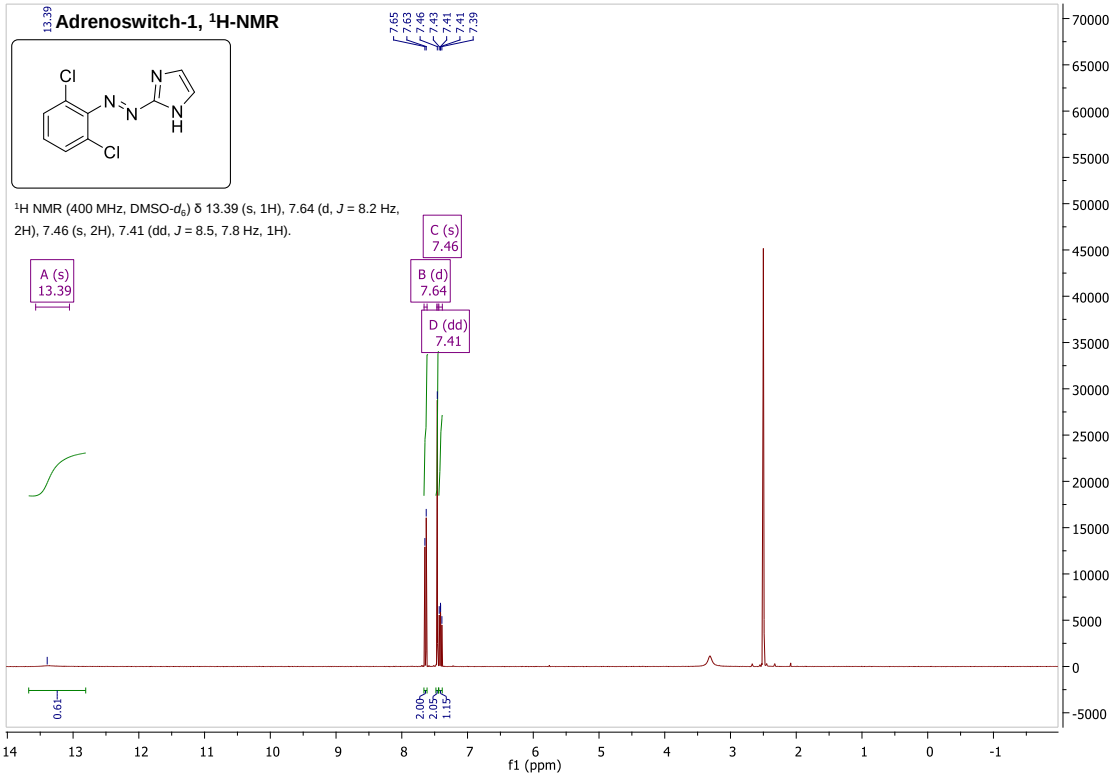

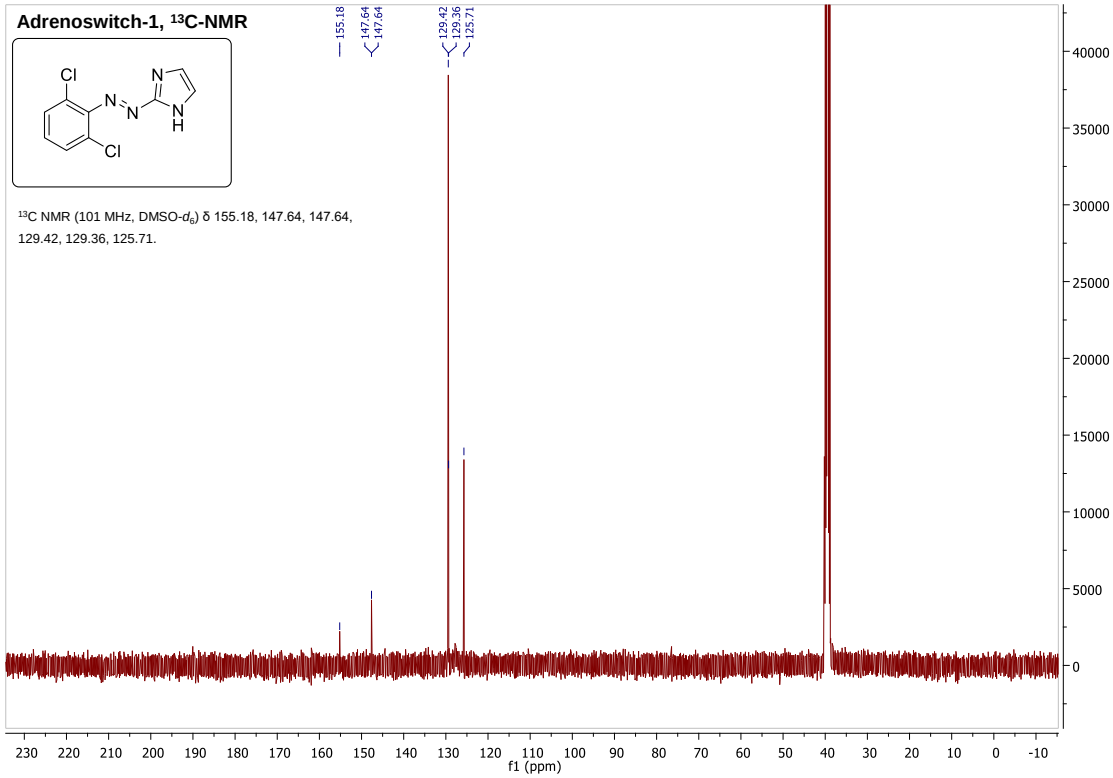

Figure S1.1 ^{1}H- and ^{13}C-NMR of adrenoswitch-1.

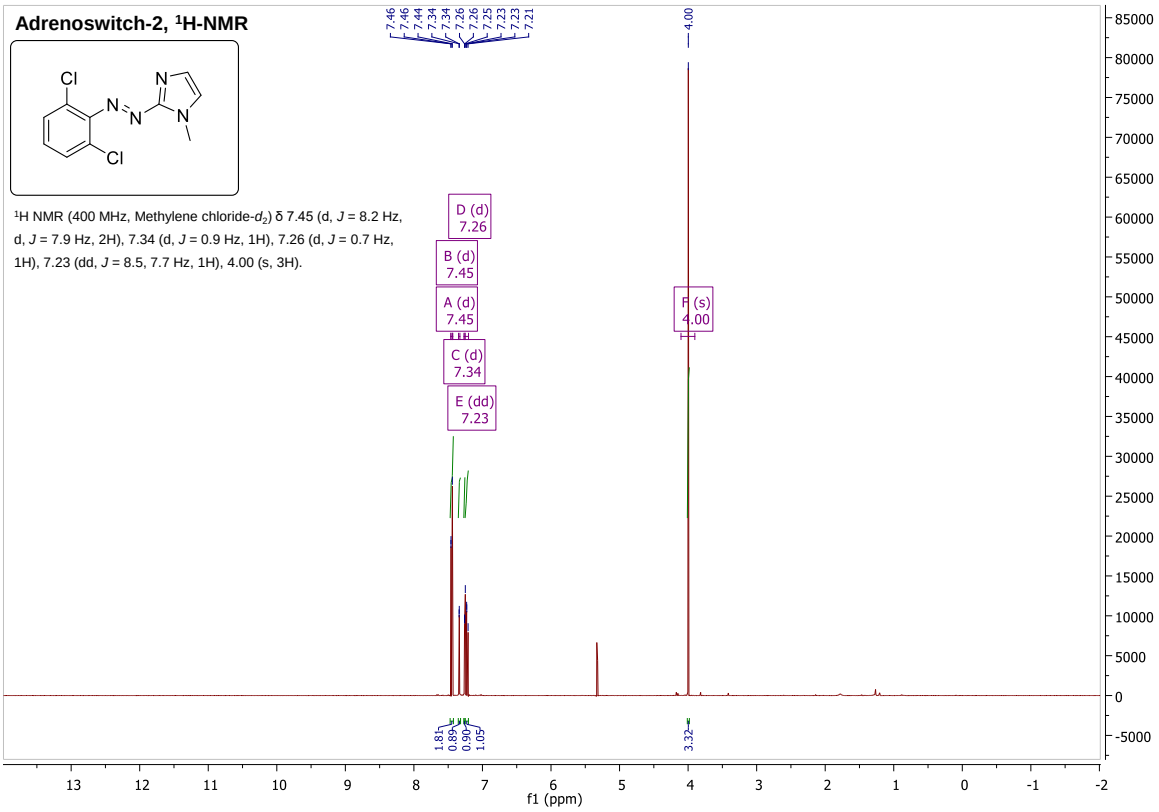

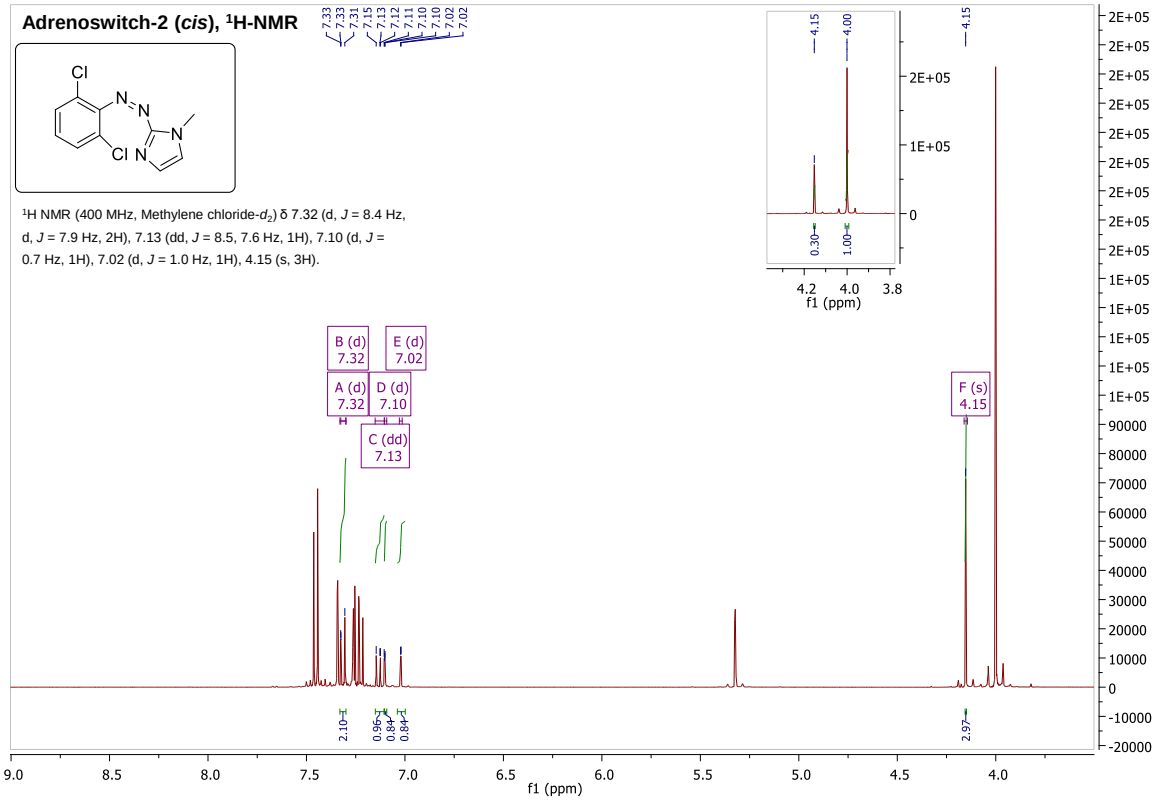

Figure S1.2 ¹H-NMR of *trans* and *cis* adrenoswitch-2.

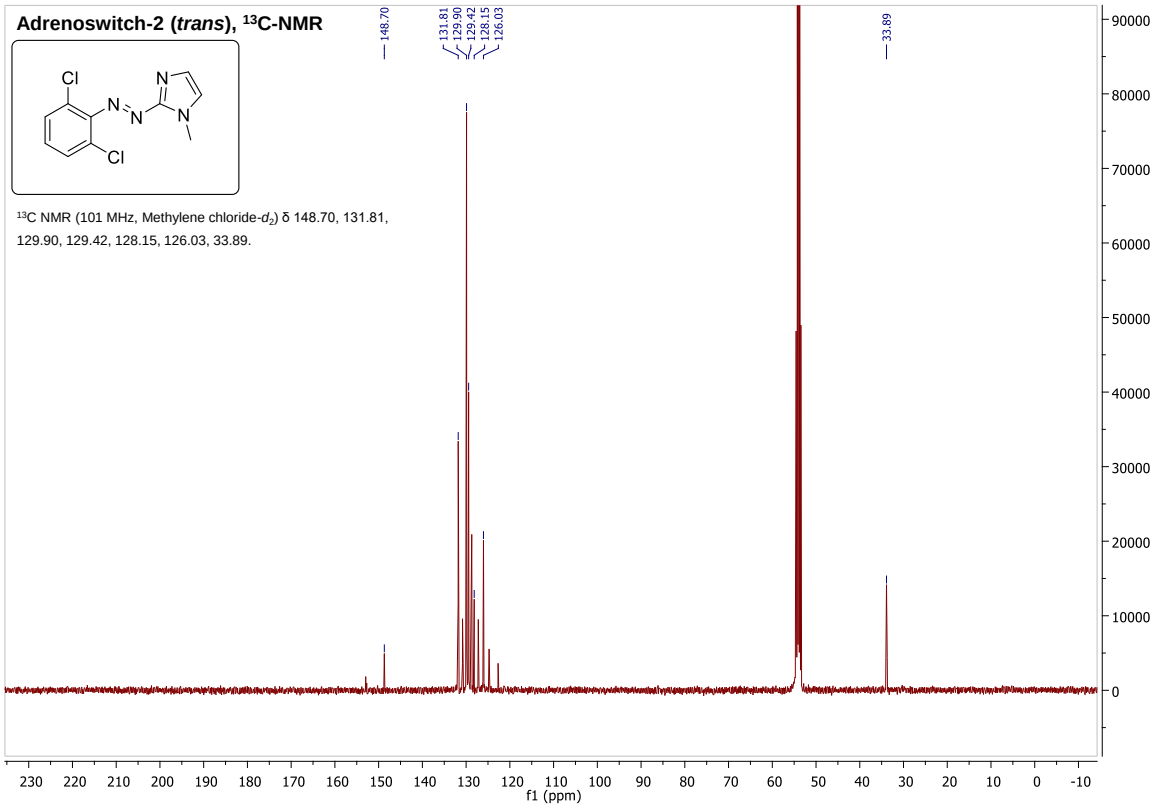

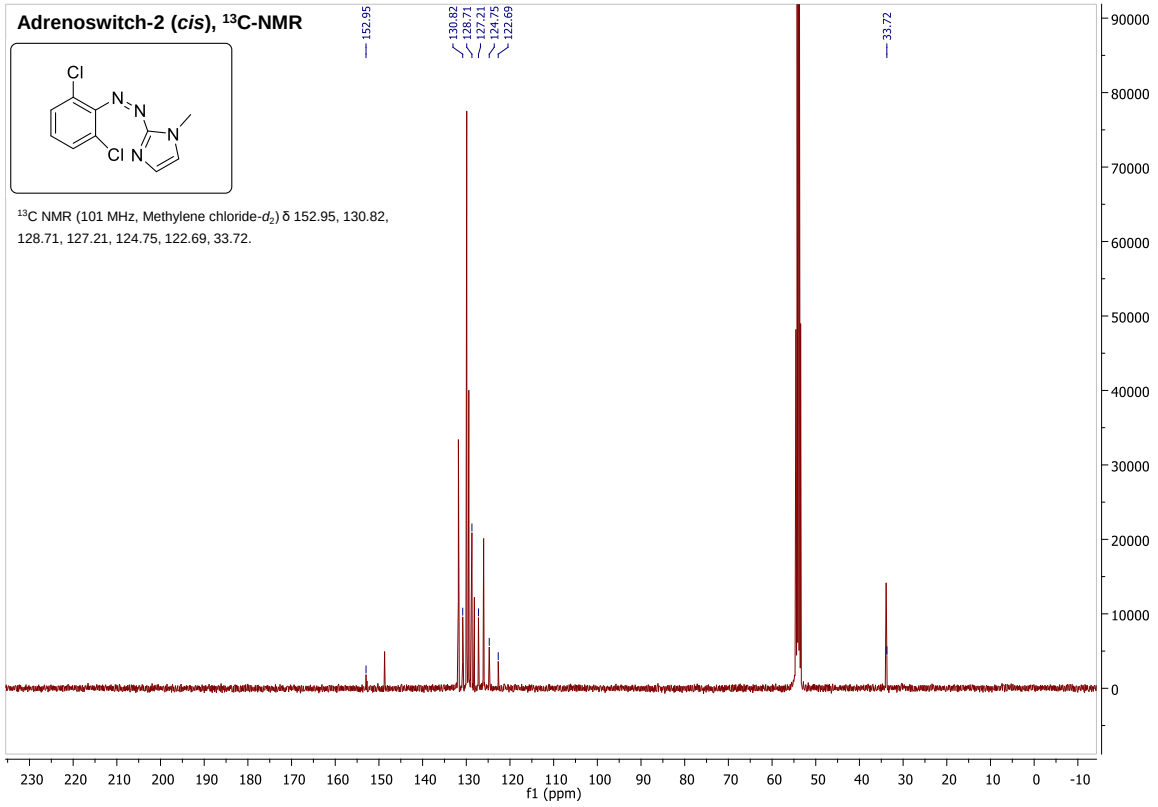

Figure S1.3 ^{13}C-NMR of *trans* and *cis* adrenoswitch-2.

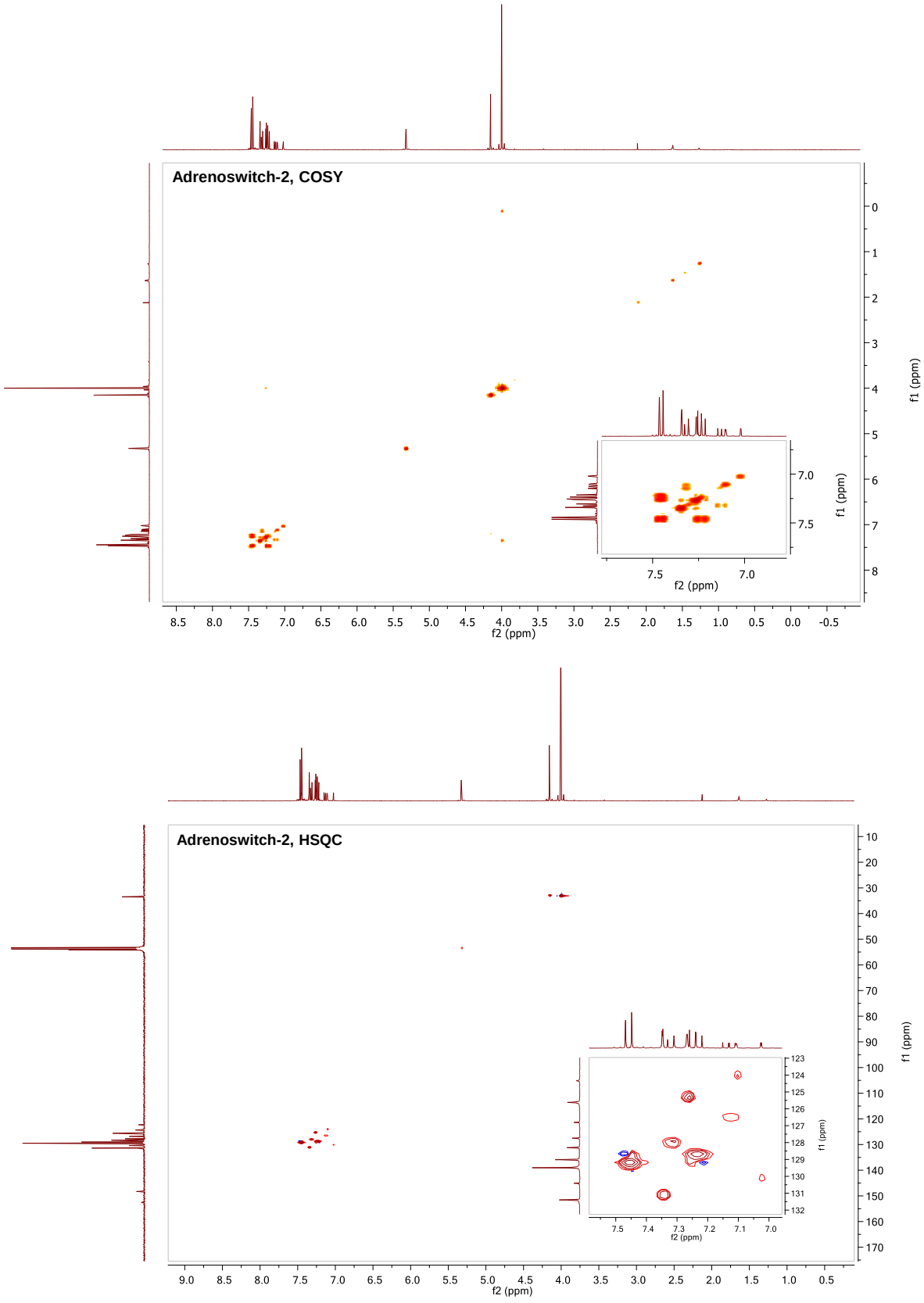

Figure S1.4 COSY and HSQC of *trans* and *cis* adrenoswitch-2.

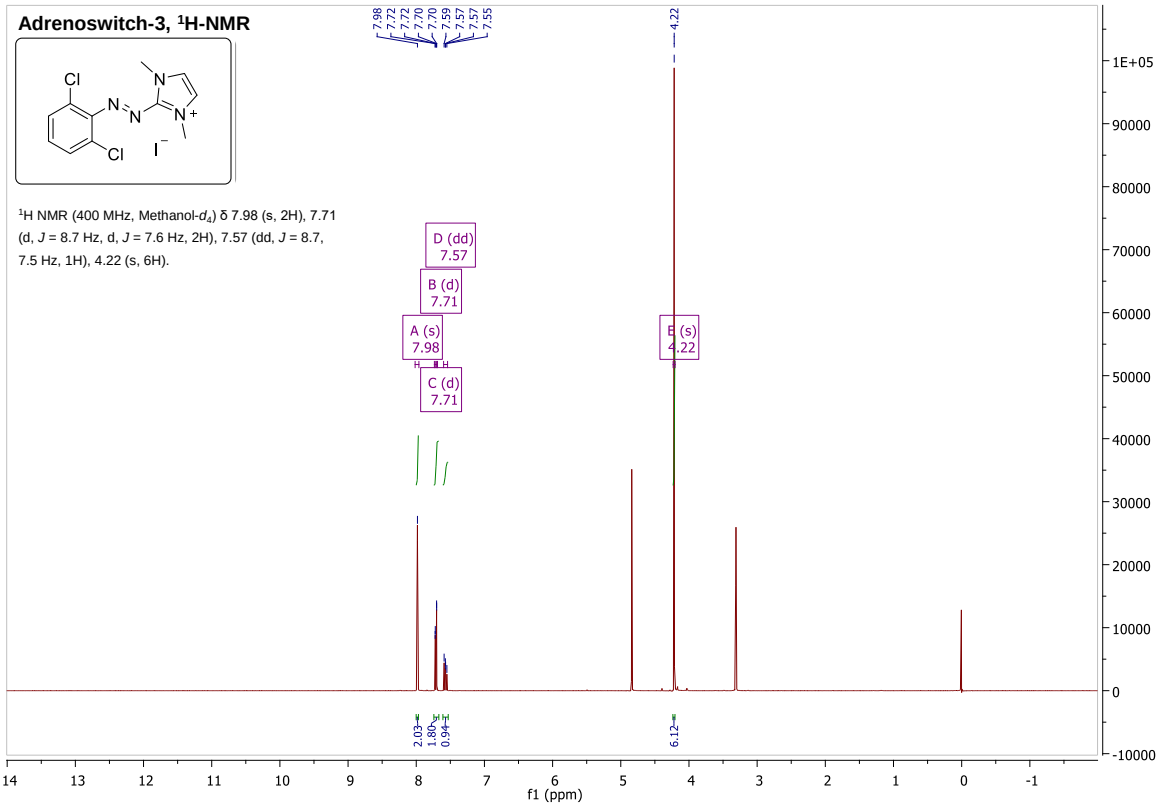

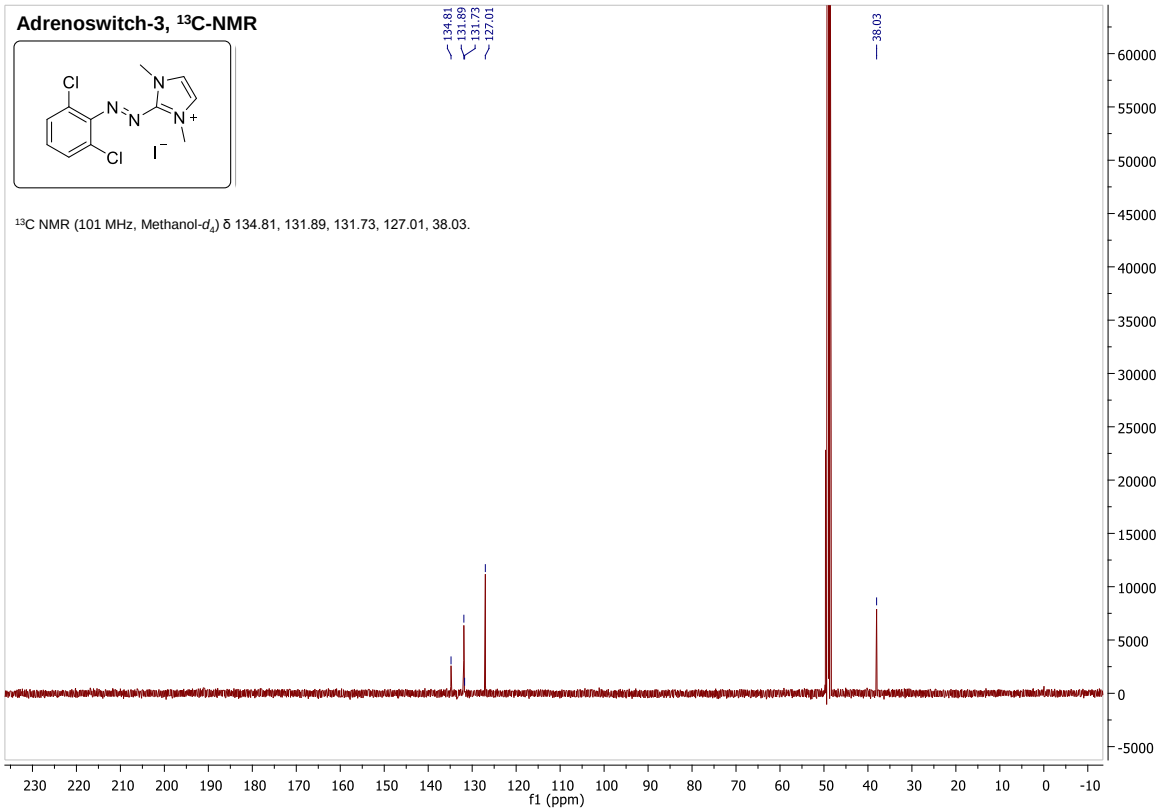

Figure S1.5 ^{1}H- and ^{13}C-NMR of adrenoswitch-3.

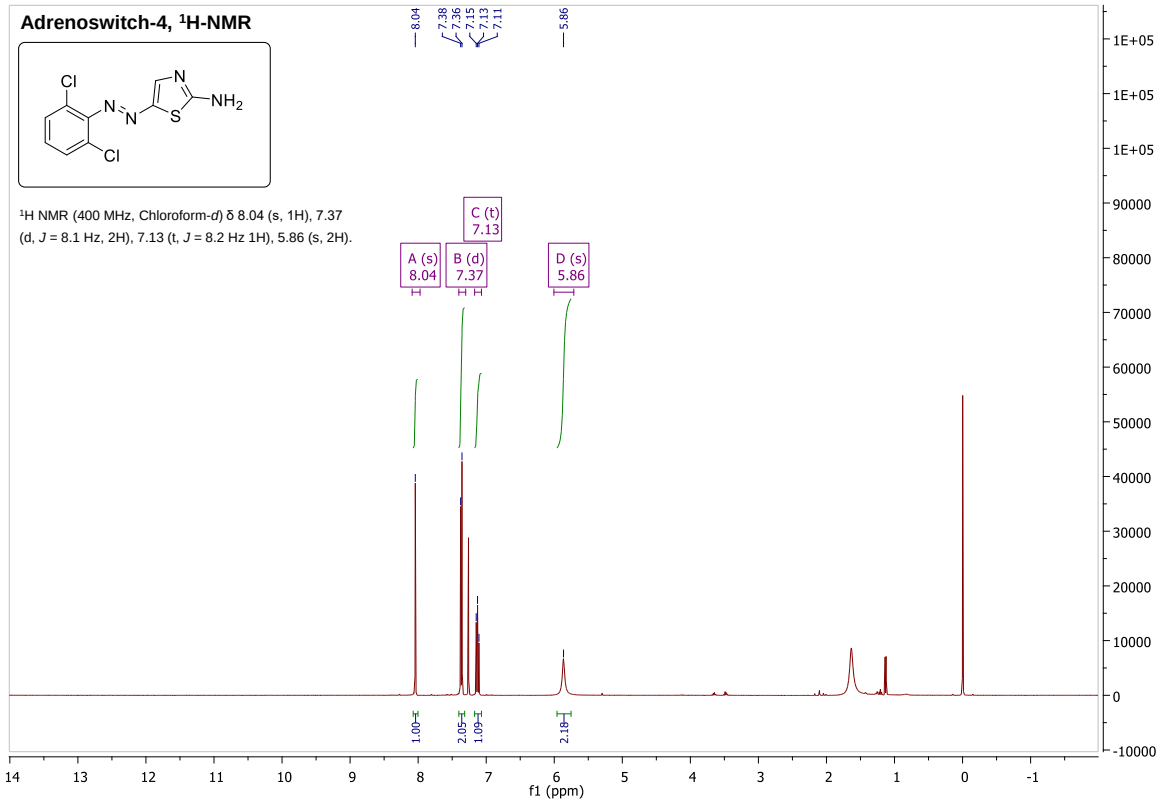

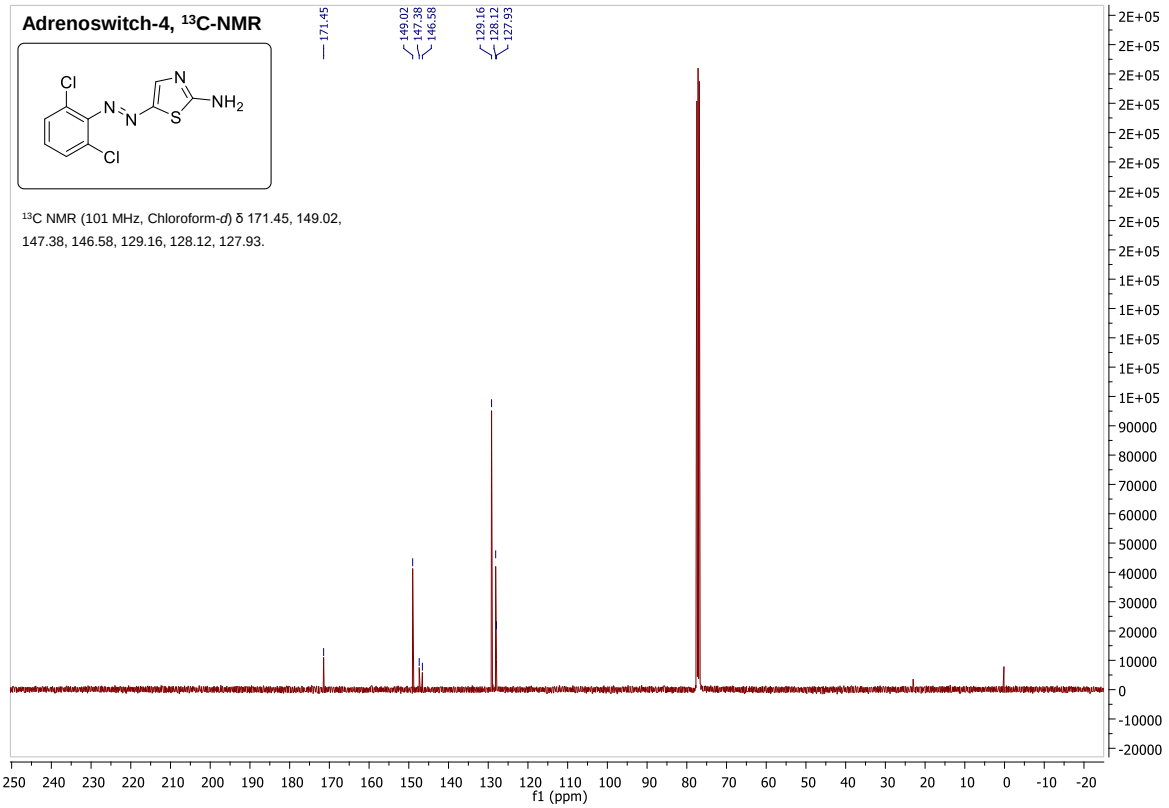

Figure S1.6 ^{1}H- and ^{13}C-NMR of adrenoswitch-4.

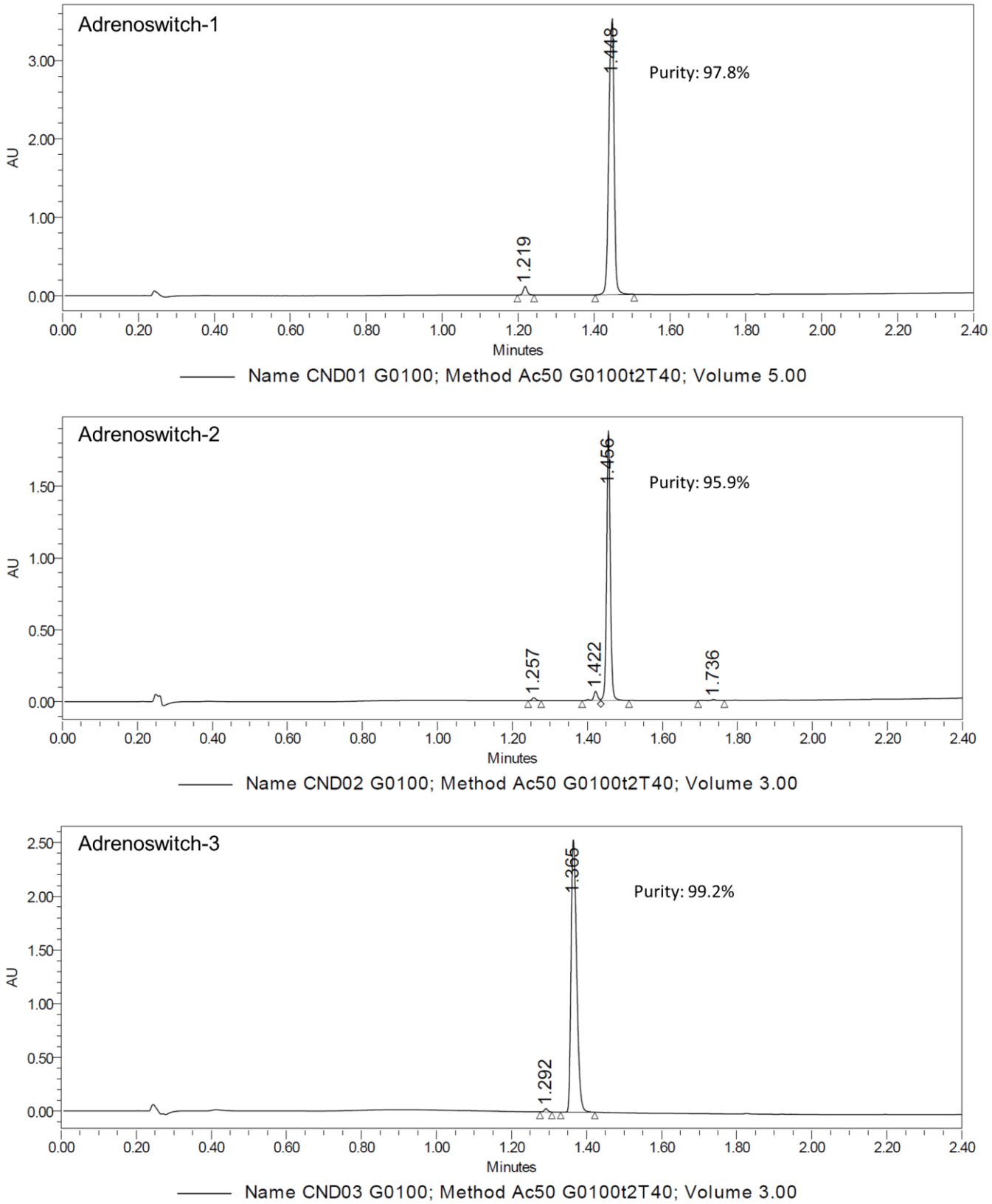

Figure S2.1 UPLC chromatograms of adrenoswitches 1-3 indicating the purity of each compound.

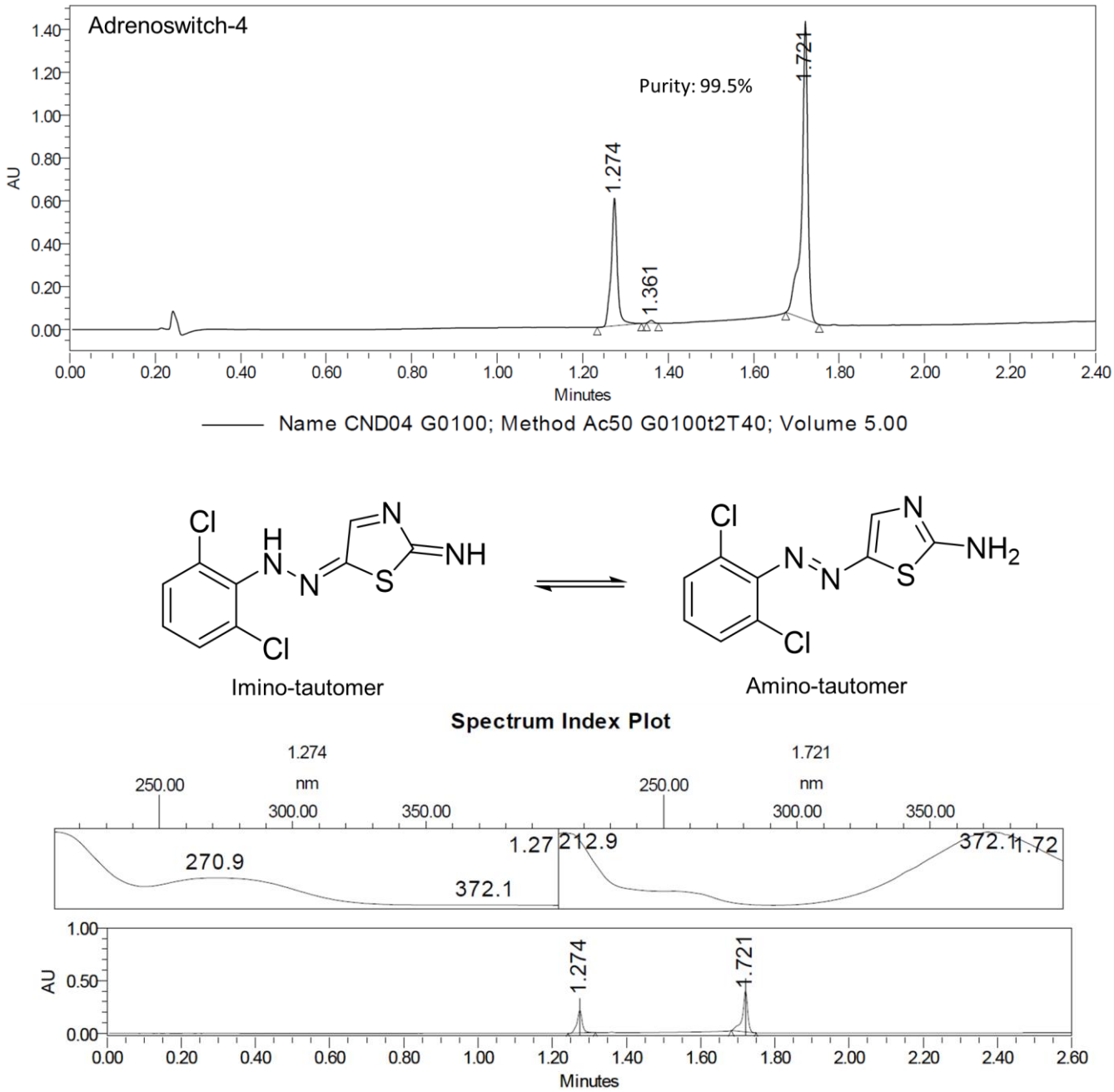

Figure S2.2 UPLC chromatogram of adrenoswitch-4 at equilibrium between its tautomeric forms (imino-tautomer at 1.274 min and *trans* amino-tautomer at 1.721 min).

Photochromic characterization

UV-Vis absorption spectra

Ultraviolet-Visible (UV-Vis) absorption spectra were extracted from UPLC chromatograms (PDA acquisition range 210-800 nm, step 1.2 nm) after having resolved the peaks of the *trans* and *cis* isomers under the analytical conditions previously described (**Figure S3.A**).

As the intensity of the absorption spectra of the two species depends on their respective concentrations, the *cis* isomer spectra of adrenoswitch-2 and -3 were corrected by normalizing the two curves at the isosbestic points in order to compare the relative intensity of the π-π^* and n-π^* transition bands (**Figure S3.C**).

Isosbestic points were determined by recording UV-Vis spectra with the spectrophotometer function of an Infinite M200 PRO Multimode Microplate Reader (Tecan, Männedorf, CH) using standard cuvette (10 mm light path). UV-Vis absorbance scans were performed under benchtop conditions (0 s, dashed curves) and at different irradiation times (380 nm) using a custom-made multi-LED dual wavelength lamp (FC Tecnics, Barcelona, ES) (**Figure S3.B**).

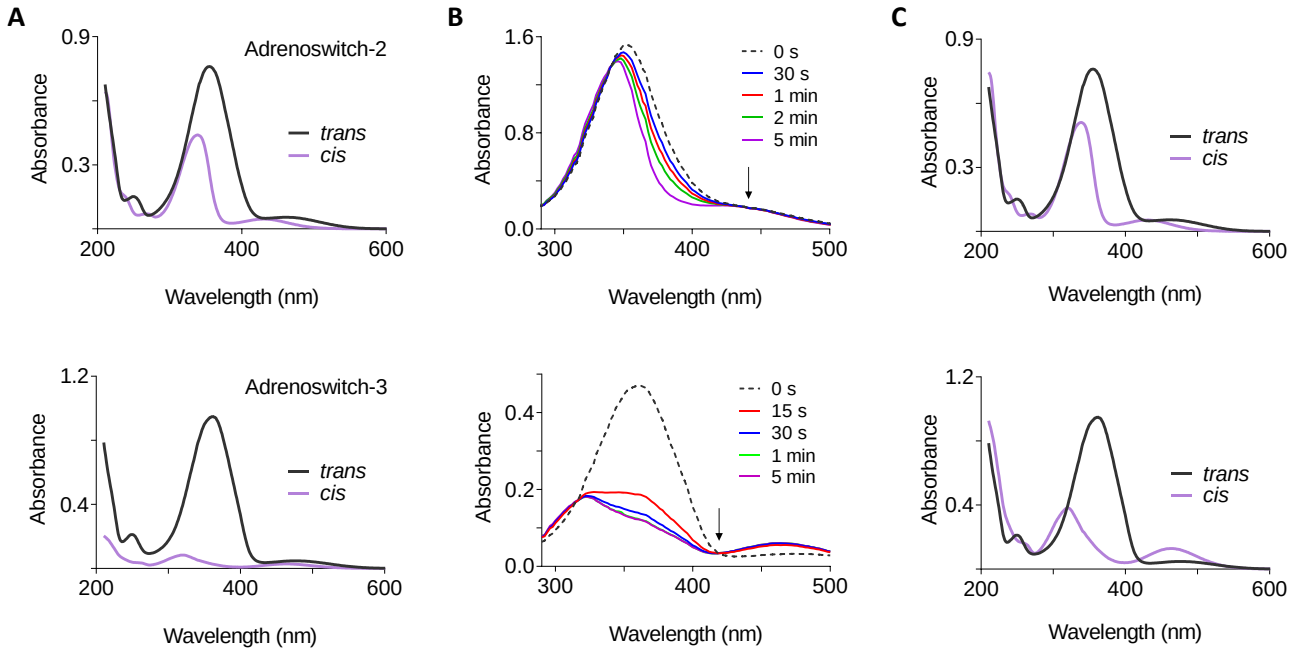

Figure S3. A) UV-Vis spectra of the pure *trans* and *cis* adrenoswitch-2 and -3 as extracted from UPLC chromatograms after having resolved the peaks of the two species with a gradient of H_2O and ACN respectively supplemented with 0.045% and 0.036% TFA (v/v). **B)** UV-Vis spectra of adrenoswitch-2 and -3 under benchtop conditions (0 s, dashed curves) and at different irradiation times under 380 nm UV light. Isosbestic points used for spectra normalization are highlighted with an arrow for both adrenoswitch-2 (441 nm) and adrenoswitch-3 (419 nm) **C)** UV-Vis spectra of the pure *trans* and *cis* adrenoswitch-2 and -3 after normalization of the curves at the isosbestic points.

Table S1. Experimental spectroscopic data and half-lives of adrenoswitches 1-4 including for both isomers the maxima of the *π-π** and *n-π** transition bands (λ_{max}) and the corresponding molar extinction coefficients (ε).

	trans isomer (*E*)				*cis* isomer (*Z*)			
	*π-π**		*n-π**		*π-π**	*n-π**	$t_{1/2}$ [f]	
	λ_{max} (nm)	ε ($10^2 M^{-1}cm^{-1}$) [c]	λ_{max} (nm)	ε ($10^2 M^{-1}cm^{-1}$) [c]	λ_{max} (nm)	λ_{max} (nm)	25°C	37°C
Adrenoswitch-1	352[a], 350[b]	138 ± 2	433[a], 432[b]	16.2 ± 0.3	- [e]	- [e]	0.267 s	- [g]
Adrenoswitch-2	355[a], 352[b]	166 ± 2	462[a], - [b, d]	- [d]	339[a]	432[a]	129 days	21 days
Adrenoswitch-3	362[a], 360[b]	154 ± 2	474[a], 472[b]	12.0 ± 0.8	320[a]	463[a]	37.0 min	15.4 min
Adrenoswitch-4	370[a], 380[b]	221 ± 3	- [d]	- [d]	- [e]	- [e]	1.65 ms	- [g]

[a] Values refer to spectra obtained from UPLC chromatograms under elution with a mixture of H_2O and ACN both supplemented with TFA (acidic conditions). [b] Values refer to spectra of the dark-adapted compounds recorded in physiological buffer (PBS, pH=7.4). [c] Molar extinction coefficients are given as means ± SD and refer to the maxima of the *π-π** and *n-π** transition bands in physiological buffer (PBS, pH=7.4) (i.e. λ_{max} values marked with [b]). [d] As the *n-π** transition band appears as a shoulder on the *π-π** band, λ_{max} and ε cannot be given. [e] Pure *cis* spectra could not be recorded due to the fast-relaxing nature of the compounds. [f] Half-lives were determined in aqueous buffer (PBS, pH=7.4). [g] Not applicable for fast-relaxing compounds.

Molar extinction coefficients

Molar extinction coefficients at a given wavelength (λ_{max}) were determined at room temperature from known concentrations of compound in physiological buffer (PBS, pH = 7.4) containing 1% DMSO. UV-Vis absorption was measured using standard cuvettes (10 mm light path) and an Infinite M200 PRO Multimode Microplate Reader from Tecan. Experiments were run in duplicates and data were analysed by linear regression with GraphPad v8.3.1 (GraphPad Software, San Diego, USA). Molar extinction coefficients are given as means ± SD (**Table S1**).

Thermal relaxation rates

Slow-relaxing adrenoswitches

Adrenoswitches-2 and -3 thermal relaxation rates were estimated by periodically monitoring absorbance at 365 nm. For each compound a 50 µM solution containing 1% DMSO was prepared in PBS (pH = 7.4) and equally split in two standard cuvettes. The compounds were isomerised under UVA light and stored in the dark either at 25˚C or 37˚C in temperature-controlled ovens (± 0.5˚C) for the whole duration of the experiment. Measurement intervals were adjusted according to the relaxation kinetics of each compound (days for adrenoswitch-2 and minutes for adrenoswitch-3). Data were analysed by nonlinear regression with GraphPad Prism v8.3.1. Half-lives were estimated using the monoexponential decay model provided by the software (**Table S1**).

Fast-relaxing adrenoswitches

Fast *cis–trans* thermal isomerization processes were studied by transient absorption spectroscopy by means of a ns LKII laser flash-photolysis spectrometer (Applied Photophysics, Surrey, UK) equipped with a Xe lamp as probe source, a monochromator, and a photomultiplier (PMT) tube (Hamamatsu Photonics, Hamamatsu, JP). Solutions

of adrenoswitch-1 and adrenoswitch-4 were excited at 355 nm (1 mJ/p) by a 20 ns pulsed laser beam arising from the third harmonic unit of a Nd:YAG Brilliant laser (Quantel, Les Ulis, FR). A 500 MHz oscilloscope (Agilent Technologies, Inc.) transferred to an Accorn PCRisk station the signal received from the PMT. The variation of absorption as measured at *t*=0 s in the 300-500 nm region mirrors the steady-state UV-Vis absorption spectra of the *trans* isomers and indicates formation of the *cis* isomers. The recovery kinetics of the photogenerated *cis* isomers were measured at 370 nm for adrenoswitch-1 and at 400 nm for adrenoswitch-4. Half-lives were determined fitting the experimental data to a monoexponential decay model with the GraphPad Prism v8.3.1 software (**Table S1**).

Photopharmacology

General methods

Animal care and experimentation conformed to the European Union (Directive 2010/63/UE) and Spanish (RD 53/2013) guidelines for the use of experimental animals. Approval was obtained from the local animal research ethics committee.

Rodents employed in the assays were maintained at constant temperature and humidity with 12-h light/dark cycles and fed *ad libitum* with standard rodent chow food and tap water.

Unless differently stated, in all the biological protocols illumination was performed with a custom-made multi-LED dual wavelength (380 nm and 500 nm) lamp (FC Tecnics, Barcelona, ES) under continuous irradiation in order to guarantee significant photoconversion even for the faster-relaxing compounds.

In vitro α_2-ARs binding assay

The affinity of adrenoswitches towards α_2-ARs was measured in human brain pre-frontal cortex membrane homogenates by competition with the α_2-AR selective radioligand [^{3}H]RX821002 (2-methoxy-idazoxan). To test *trans* adrenoswitches, the molecules and the incubation mixtures containing the compounds were kept in the dark prior to and during the whole duration of the experiment till displacement of the radioligand had occurred and the membranes had been filtered. Binding data for the *cis* isomers were obtained by exposing the samples to continuous UV irradiation during incubation period. Light-induced artifacts were discarded using α_2-AR agonist clonidine as control. The results are expressed as pIC_{50} values and presented in **Figure S4.B**.

Materials and methods

Drugs

Drugs were purchased from Sigma (St. Louis, USA) and were of the highest purity commercially available. [^{3}H]RX821002 (NET1153, lot number 2203743, specific activity 36.5 Ci/mmol) was obtained from Perkin Elmer (Waltham, USA).

Membranes preparation

Neural membranes (P2 fractions) were prepared from prefrontal cortex of human brain. *Post-mortem* human brain samples were obtained at autopsies in the Instituto Vasco de Medicina Legal, Bilbao, Spain, in compliance with policies of research and ethical boards for *post-mortem* brain studies. Samples from 6 different subjects (~

1 g each) were pooled and homogenized using a Teflon-glass grinder (10 up-and-down strokes at 1500 rpm) in 10 volumes of homogenization buffer (1 mM $MgCl_2$, and 5 mM Tris-HCl, pH 7.4) supplemented with 0.25 M sucrose.

The crude homogenate was centrifuged for 5 min at 1000 × g (4˚C). The supernatant was removed and centrifuged again for 10 min at 40000 × g (4˚C). The resultant pellet was washed twice in 5 volumes of washing buffer (50 mM Tris-HCl, pH 7.5) and re-centrifuged in similar conditions. Protein content was measured according to the Bradford method using Bovine Serum Albumin (BSA) as standard, and aliquots of 1 mg protein were stored at -70˚C until assay.

Radioligand competitive binding assay

Specific [^{3}H]-RX821002 binding was measured in a final incubation volume of 250 µL (50 mM Tris-HCl, pH 7.5) with 90 µg of protein/well in 96-well plates. Membranes were incubated with [^{3}H]-RX821002 (2 nM) for 30 min at 25°C and 450 rpm in the absence or presence of the competing compounds (11 concentrations over the range 10^{-10} – 10^{-3} M). Incubations were terminated by separating excess free ligand from membrane-bound ligand by rapid filtration under vacuum (1450 Filter Mate Harvester, PerkinElmer) through GF/C glass fibre filters pre-treated with 0.5% polyethylenimine (PEI). The filters were then rinsed three times with cold incubation buffer, air-dried (120 min), and counted for radioactivity by liquid scintillation spectrometry using a MicroBeta TriLux counter (PerkinElmer). Nonspecific binding was determined in the presence of adrenaline (10^{-5} M). Specific binding was determined and plotted as a function of the compound concentration.

Data analysis and statistics

Analysis of competition experiments were performed by nonlinear regression using the GraphPad Prism v8.3.1 software (GraphPad Software, San Diego, USA). All experiments were analysed assuming a one-site model of radioligand binding. Results are from two independent experiments each run in either duplicates or triplicates. Adrenoswitches binding potencies were expressed as the negative logarithms of the concentrations inhibiting 50% of the radioligand binding (pIC_{50} ± SD). Statistical differences between two means were determined by Student's *t* test for unpaired observations. *P* values less than 0.05 were considered to indicate statistically significant differences.

A

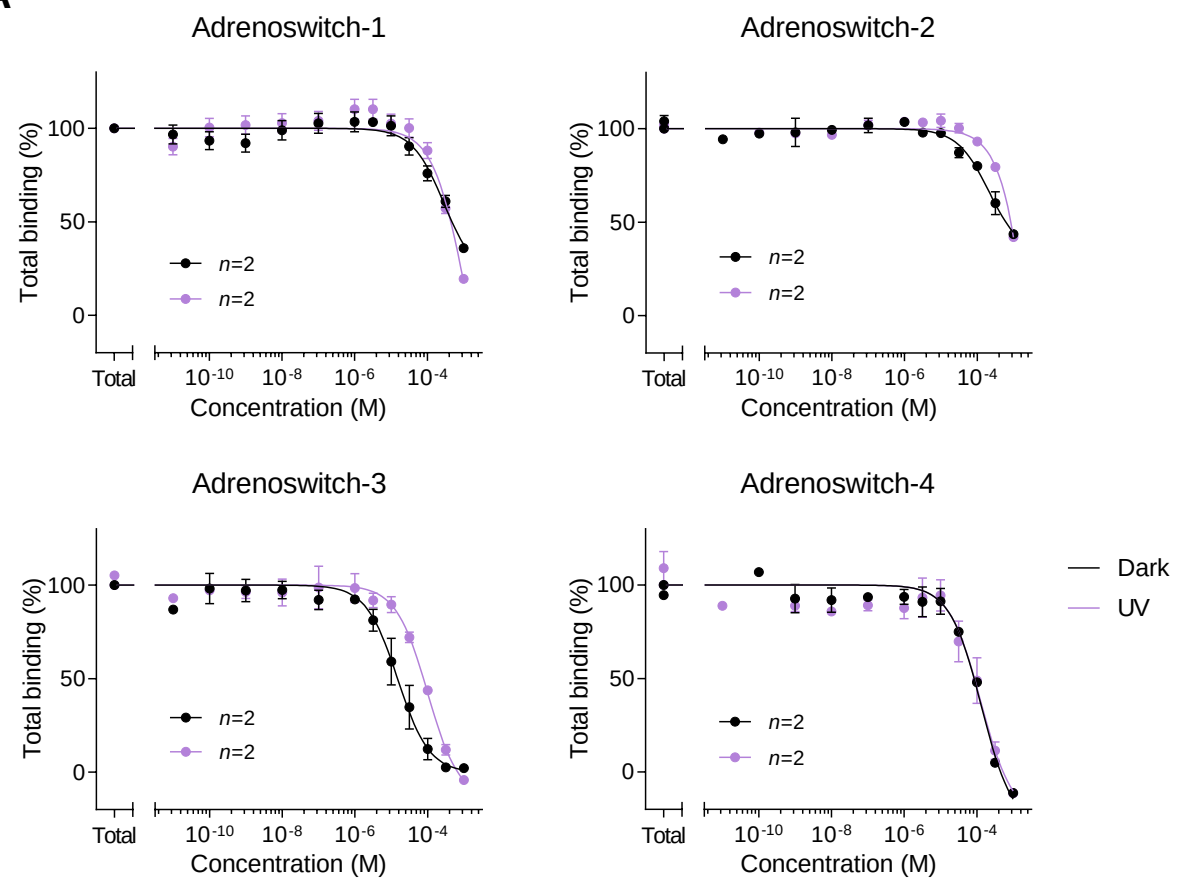

B

Binding potency to α_2-ARs [pIC_{50} ± SD]		
	Dark	**UV**
Clonidine	7.5 ± 0.1	7.6 ± 0.1
Adrenoswitch-1	3.4 ± 0.2	3.4 ± 0.2
Adrenoswitch-2	3.3 ± 0.2	3.0 ± 0.2 ***
Adrenoswitch-3	4.8 ± 0.1	4.1 ± 0.1 ***
Adrenoswitch-4	4.1 ± 0.1	4.1 ± 0.2

Figure S4. A) Comparison of competition binding curves of dark-relaxed (*trans*, in black) and UV-illuminated (*cis*, in violet) adrenergic photoswitches to α_2-ARs in human brain pre-frontal cortex tissue. Binding is expressed as percentage of radioligand - [^{3}H]RX821002 - bound to the receptor in the presence of the competitor. Data are means ± SEM of two independent experiments run in duplicates or triplicates. **B)** Table comparing the binding potency parameters obtained from non-linear analysis of competition binding experiments for the reported compounds in their dark-adapted form or under UV-illumination. Values, expressed as pIC_{50}, are means ± SD; statistically significance differences are indicated with *** ($p \leq 0.001$).

Ex vivo electromyography on isolated rat aorta

Drugs

Phenylephrine hydrochloride (PE), carbachol (Cch) and N^G-methyl-L-arginine acetate salt (L-NMMA) were purchased from Sigma (St. Louis, USA) and were of the highest purity commercially available. Stocks solutions of PE, Cch and L-NMMA were prepared in deionized water, while the reported compounds (Adrenoswitch-1 – 4) were dissolved in DMSO and diluted in the same solvent. Concentrations are expressed as final molar concentrations after addition of the compounds to the organ chamber solution. The total concentration of DMSO in the organ baths did not exceed 1% after cumulative additions of the adrenergic photoswitches.

Tissue preparation

Aortic rings were obtained from male Wistar rats (350-460 g). In preparation to the experiment, rats were euthanized with an overdose of 4-5% inhaled isoflurane and exsanguination. The descendent thoracic aorta was excised, immediately placed in ice-cold Krebs-Henseleit solution (composition in mM: NaCl 119; KCl 4.7; $MgSO_4$ 1.2; KH_2PO_4 1.2; $CaCl_2$ 1.6; $NaHCO_3$ 24; glucose 11; EDTA 0.026, pH 7.4) and carefully freed of any fat and connective tissue. The tissue was cut in 4 mm segments which were studied in parallel in organ chambers.

Isometric tension measurement

Each ring was suspended by two stainless steel hooks passed through its lumen in 25-ml organ bath chambers equipped with isometric force transducers, micro positioners and a thermo regulated pump (Letica, PanLab, Barcelona, ES). Each chamber was filled with 20 ml Krebs-Henseleit solution, maintained at 37°C and continuously aerated with 5% CO_2/95% O_2. Changes in isometric tension were recorded with a ML866 PowerLab 4/30 data acquisition system and the LabChart v7.3.7 software (ADInstruments, Castle Hill, AUS). Aortic rings were stretched to a resting tension of 1500 mg and allowed to equilibrate for 60 min in fresh Krebs-Henseleit solution before receiving any drug. After stabilization, evidence of functional endothelium was obtained by adding 10^{-5} M Cch to rings precontracted with 10^{-6} M PE. The endothelium was considered viable when relaxation to the muscarinic agonist was 50% or greater. Subsequently, vessels were thoroughly washed with fresh Krebs-Henseleit solution, allowed to rest and stabilize for 30 min, and then incubated for other 30 min in the presence of 10^{-3} M L-NMMA. The aortic rings were again pre-contracted with 10^{-6} M PE and when the response to the adrenergic agonist had stabilized, relaxation dose-response curves were constructed by stepwise cumulative addition of the adrenergic photoswitches. Each ring was used to build a single dose-response curve. *Cis* isomers were tested by illuminating the organ baths with a UV led plate (380 nm) taped sideways so to orthogonally irradiate the whole chambers volume. UV light was switched on once the vasoconstrictive response to PE had reached its *plateau* and the irradiation was maintained throughout the whole duration of the dose-response curve. Adrenergic photoswitches were added as soon as the spontaneous vasodilatory response to UV light had recovered and stabilized. For both *trans* and *cis* isomers, a total of 12 doses was tested, initially increasing the compounds concentration 10-fold at each step and eventually reducing it to a 2-3-fold increase when closer to the EC_{50}. Each addition was made only after the response to the previous one had remained steady at its maximum. However, the response to adrenoswitch-4 showed an extremely slow kinetic, perhaps indicating a different mechanism of action and rendering impossible reaching a clear saturation for each of the tested doses. In this case, potencies of the *trans* and *cis* isomers were compared measuring relaxation achieved under dosing patterns with identical timing. Controls for time-dependent spontaneous relaxation were randomly performed in parallel with the experimental

rings. Control vessels did not receive any drugs after tonus had been induced with PE. Spontaneous relaxation was either absent or no greater than 9% per hour without exceeding 28% over the average course of the experiment. All experiments were carried out under no illumination apart from the one required for *cis*-isomerization when so intended.

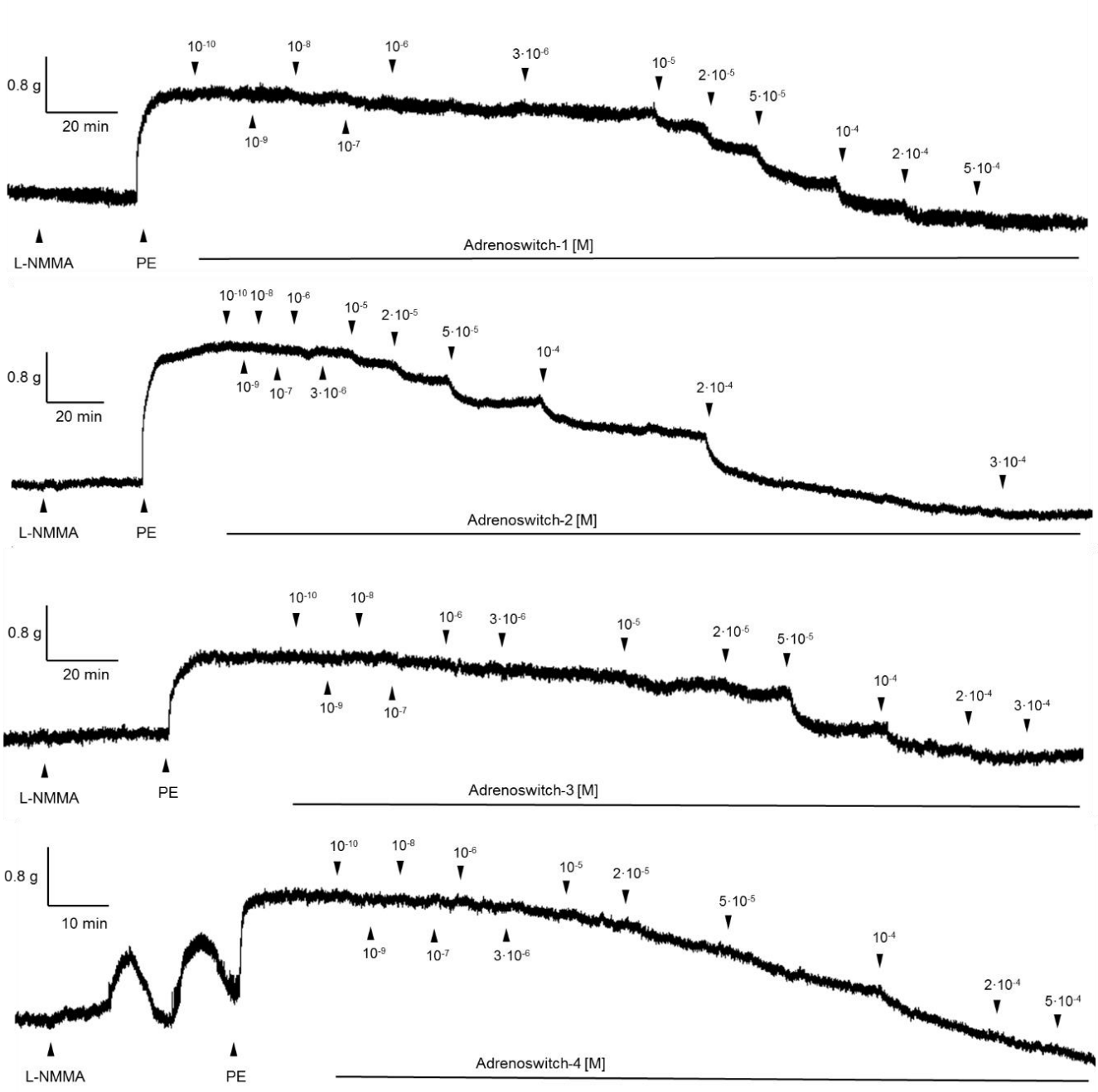

Figure S5. Representative traces showing the change in tension over time of rat aortic rings pre-contracted with PE (10^{-6} M) in the presence of L-NMMA (10^{-3} M) and allowed to relax under dark conditions in response to cumulative doses of the reported adrenergic photoswitches. Drugs addition is marked by an arrow and the doses indicated in M.

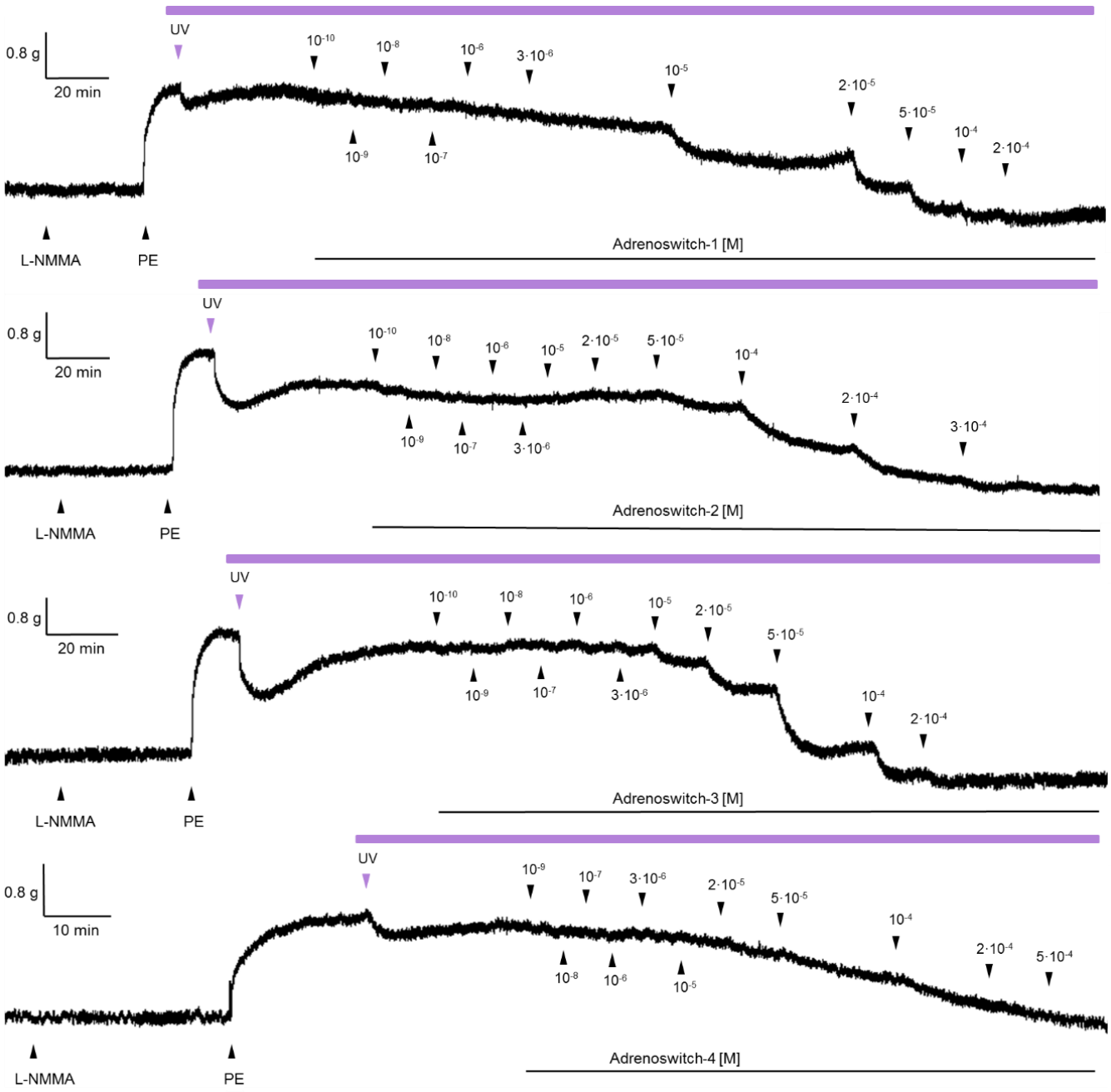

Figure S6. Representative tension-versus-time graphs showing UV-light induced relaxation of rat aortic rings pre-contracted with PE (10^{-6} M) in the presence of L-NMMA (10^{-3} M). After having stabilized, the rings were allowed to relax in response to cumulative doses of the reported adrenergic photoswitches while UV irradiation was maintained. Drugs addition and UV light application are marked by an arrow and the doses indicated in M.

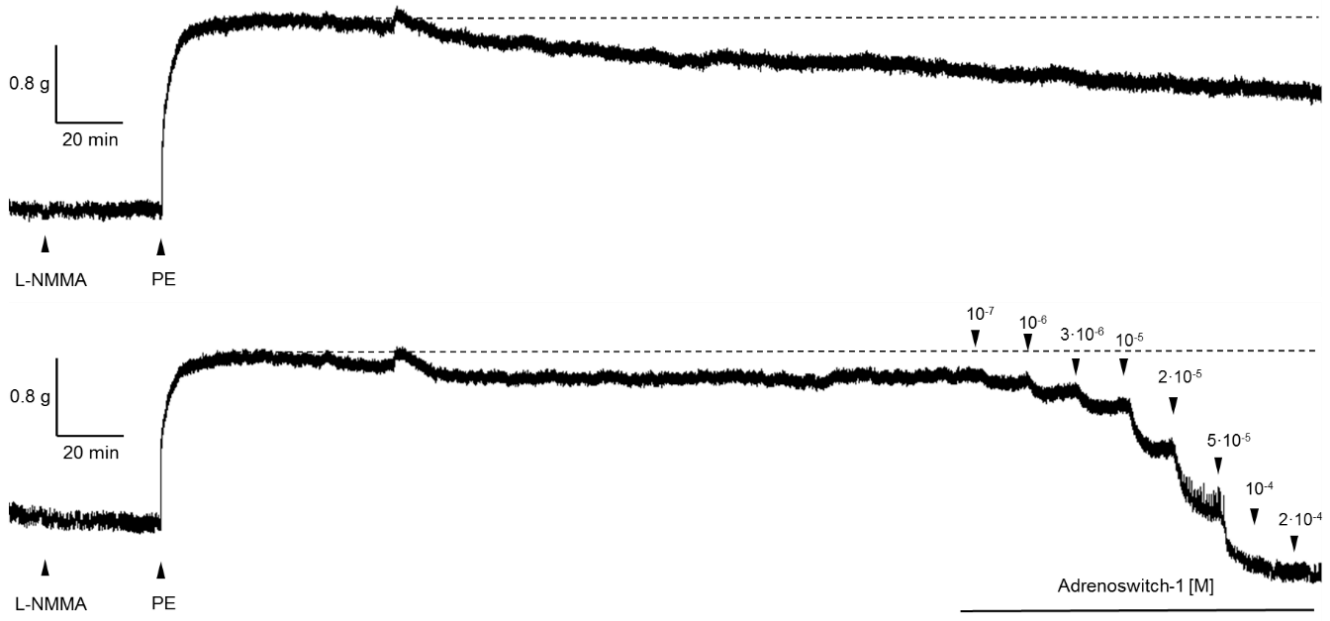

Figure S7. Representative traces showing the degree of spontaneous time-dependent relaxation observed over a course of 5 hours. Rat aortic rings were pre-contracted with PE (10^{-6} M) while in the presence of L-NMMA (10^{-3} M). Maximal response to the adrenergic agonist is indicated by a dashed line. Preparations that showed minimal loss of tension were eventually allowed to relax in response to cumulative doses of one of the reported adrenergic photoswitches to verify their integrity. Drugs addition is marked by an arrow and the doses indicated in M.

Data analysis and statistics

Relaxations were expressed as percentages of the reference contractions to PE. All experiments were analyzed using the statistical software GraphPad Prism v8.3.1. Data were normalized and fitted by nonlinear regression to three parameters dose-response curves. The results are expressed as means ± SEM, with *n* representing the number of animals. Vasodilatory potency of the different adrenoswitches was given for both the dark and UV-irradiated forms as the negative logarithm of the concentration producing a half-maximal response pEC_{50} ± SD. Statistical differences between two means were determined by Student's *t* test for unpaired observations. *P* values less than 0.05 were considered to indicate statistically significant differences.

A

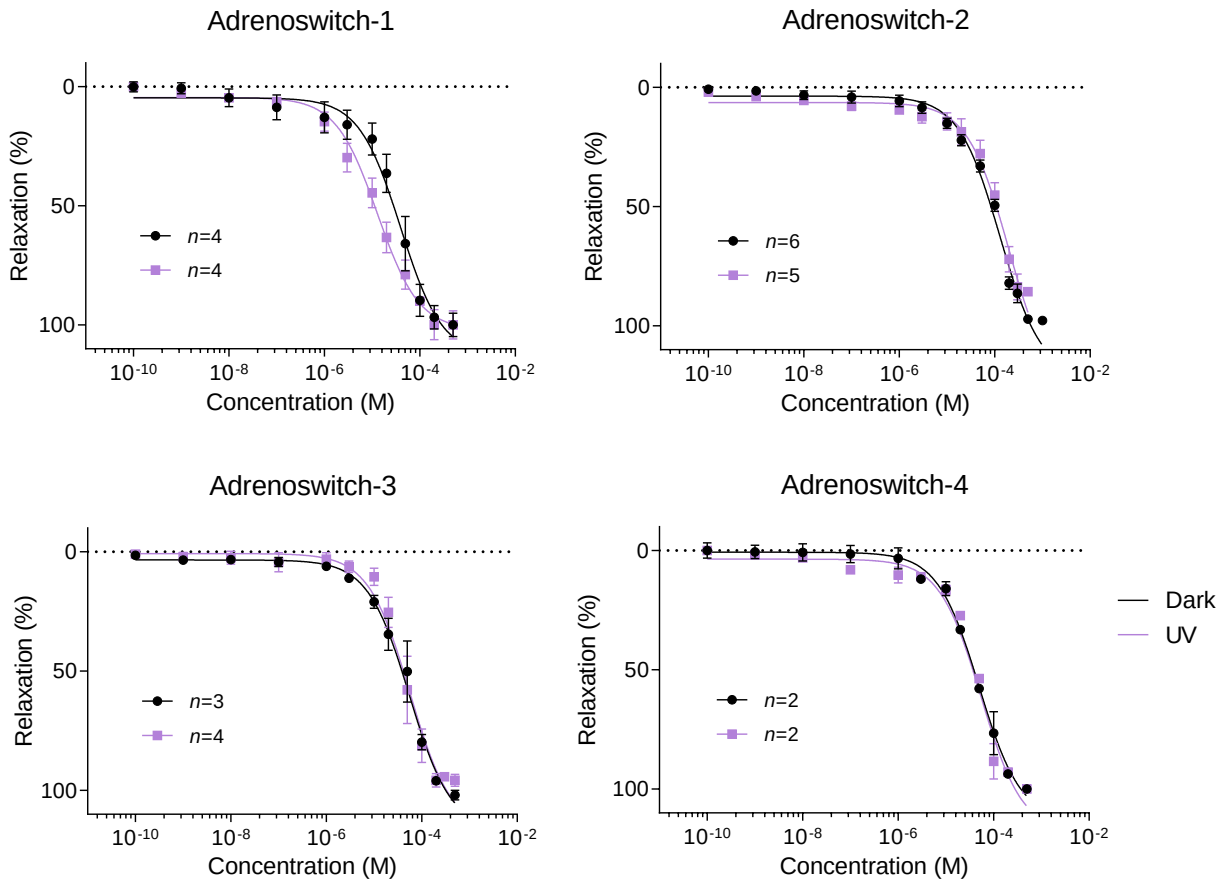

B

Vasodilatory potency on pre-contracted aortic rings [pEC_{50} ± SD]		
	Dark	**UV**
Adrenoswitch-1	4.41 ± 0.09	4.89 ± 0.06 ****
Adrenoswitch-2	3.89 ± 0.05	3.7 ± 0.1
Adrenoswitch-3	4.26 ± 0.06	4.25 ± 0.08
Adrenoswitch-4	4.30 ± 0.07	4.27 ± 0.09

Figure S8. A) Comparison of logarithmic dose-response curves to dark-relaxed (*trans*, in black) and UV-illuminated (*cis*, in violet) adrenergic photoswitches administered to aortic rings pre-contracted with PE and previously treated with L-NMMA. Relaxation is expressed as percentages of the reference contraction induced by PE. Data are means ± SEM, with *n* representing the number of animals. **B)** Table comparing the vasodilator potency of the reported compounds in their dark-adapted form or under UV-irradiation. Values, expressed as pEC_{50}, are means ± SD; statistically significance difference are indicated with **** ($p \leq 0.0001$).

In vivo photomodulation of zebrafish locomotion activity

Animal housing

Wild-type zebrafish embryos (Tupfel long-fin strain, *Danio rerio*) were purchased from the animal facility of the Barcelona Biomedical Research Park (PRBB) and raised in darkness for 6 days at 28.5°C in sterilized tap water. Petri dishes housing the animals were cleaned and replenished with fresh water on a daily basis. Animal development was checked every 24 hours. Unhealthy or abnormal embryos and larvae were removed and euthanatized in tricaine methanesulfonate 0.02%.

General methods for locomotor assays

Behavioral studies were conducted on wild-type zebrafish larvae at 7 days post-fertilization (7 dpf). Vehicle and compounds were added with a multichannel pipette to exclude differences due to delays in the application of each solution. Movements were recorded and analyzed using the ZebraBox tracking system and the ZebraLab software (ViewPoint Life Science, Lyon, FR). On the morning of the assay, 7 dpf larvae were moved into a new batch of fresh water and checked for motility capabilities and possible physical mutations. Larvae were then randomly divided into control and treatment groups. Each individual was placed in a separate well of a 96-well plate, each containing 200 µl of fresh sterilized water and left undisturbed in the dark for 40 min to get acquainted with the new setting (habituation time). Afterwards, 100 µl of water were removed from each well and replaced with 100 µl of a double concentrated vehicle or treatment solution. At this point, the plate was inserted into the ZebraBox and the recording period started. In the different protocols, illumination at 365, 380, 455 and 500 nm was performed with a built-in array of 12 LEDs placed 12 cm away from the multiwell plate. Light intensity, measured with a Newport 1916-C optical power meter coupled to a Newport 918D-SL-OD3R detector (Newport Corporation, Irvine, USA) for 365 nm, 380 nm, 455 nm, and 500 nm were 5.9 $mW \cdot cm^{-2}$, 0.2 $mW \cdot cm^{-2}$, 2.4 $mW \cdot cm^{-2}$ and 0.7 $mW \cdot cm^{-2}$, respectively. All experiments were conducted at 12.00 pm (UTC+01:00).

Protocol 1 (Figure S9)

Activity was recorded for a total of 48 min. Animals were exposed to sequential cycles of UV light followed by darkness or visible light. Illumination wavelengths and concentrations used are detailed for each adrenoswitch in the results discussion. For all the compounds the illumination protocol was the following: darkness (20 min for adaptation, named relaxation period), 3 cycles of UV (1 min) followed by darkness or visible light (1 min), 3 cycles of UV (2 min) followed by darkness or visible light (2 min) and 5 min of UV followed by 5 min in the dark or under visible light.

Protocol 2 (Figure S10)

As some compounds displayed time-dependent effects (e.g. **Figures S9.A-D**), they were difficult to characterize with sequential illumination. In order to perform time-resolved zebrafish activity experiments simultaneously under UV-illuminated and non-illuminated conditions, we covered a section of the multiwell plate with a UV-Vis filter (IR780C, Shanghai Visualplas Co. Ltd). The filter cut band over 780 nm transmits infrared (IR) light to the ZebraBox built-in camera thus allowing recording of the movements. Non-illuminated wells are indicated in the text and figures as “UV-Vis filter”. Larvae swimming activity was recorded for a total of 40 minutes: the first 20 minutes under 365 nm UV illumination (with and without UV-Vis filter to study in parallel the effects of *cis* and *trans* adrenoswitch-1, respectively) and the remaining 20 minutes in the dark to evaluate recovery of the animals.

Tracking and analysis of swimming activity

Alterations of locomotor activity were determined by monitoring and measuring fast movements, swimming distances and duration of high-speed swimming. In particular, the dependent variables measured included: distance travelled at ≤ 2 $mm \cdot s^{-1}$, distance travelled at 2-6 $mm \cdot s^{-1}$, distance travelled at ≥ 6 $mm \cdot s^{-1}$, time spent moving, time spent freezing, and number of bursts. The arbitrary cut-off for motility (6 $mm \cdot s^{-1}$) was chosen because no false positives due to image treatment were found in contrast to lower movement thresholds. Total movements were not considered to limit the error of the video recording on minimal movements. All experiments were analyzed using the statistical software GraphPad Prism v8.3.1 and results are represented as means ± SEM. Statistical differences were determined by two-way ANOVA with Tukey's multiple comparison test. *P* values less than 0.05 were considered to indicate statistically significant differences.

Results discussion

For the screening of the adrenoswitch derivatives (1-4, **Figures S9.A-D** respectively), 7 dpf larvae were monitored for a total of 48 minutes under different illumination conditions depending on the photochemical properties of each compound. Adrenoswitch-1 and -4 were illuminated with 365 nm UV light for *trans* to *cis* isomerisation, needing no secondary illumination to revert from *cis* to *trans* due to their very fast-relaxing properties. On the other hand, adrenoswitch-2 was previously illuminated at 365 nm for *cis*-isomerisation followed by illumination with blue light (455 nm) in order to recover the *trans*-isomer. Finally, adrenoswitch-3 was illuminated with UV (380 nm) and green (500 nm) light for *cis*- and *trans*-isomerisation, respectively. Clonidine (**Figures S9.A-B**, green traces) was used as a control in the analysis and study of larvae motility affections. As it can be observed in **Figures S9.A-B**, clonidine (50 µM) hastily decreased larvae movements during the first 20 min of darkness (relaxation period, RP). Its inhibitory effect was only marginally affected by concomitant illumination changes, in contrast to vehicle-treated animals (dark traces), which maintained both basal motility and their photomotor response (PMR) during the whole duration of the experiment. Adrenoswitch-1 (**Figure S9.A**) significantly increased larvae swimming distances during RP, but then their locomotor activity started to decay towards levels comparable to clonidine as illumination cycles added up over time. We postulated that this increasing sedation was a result of adrenoswitch-1 getting activated by repeated exposure to UV cycles and that the inhibitory effect on zebrafish locomotion was appreciable only in the dark, because otherwise masked by the animal photomotor response to UV light. Our hypothesis was later confirmed by means of a specifically designed time-dependent experiment, where we could simultaneously evaluate drug activity under UV-illuminated and non-illuminated conditions (**Protocol 2**, **Figures S10.A-B**). A sedative effect could be observed also for adrenoswitch-4 (**Figure S9.D**), however the compound showed no photoswitchable activity despite its potency and rapid on-set of action. In comparison to the other derivatives, adrenoswitch-2 (**Figure S9.B**) acted differently on larvae motility. During UV illumination, motility decreased to levels comparable to clonidine and recovered only when visible light was applied, showing a robust and above startle response. Lastly, adrenoswitch-3 treated larvae (**Figure S9.C**) highlighted no significant differences from vehicle-treated larvae, neither under UV nor under visible illumination.

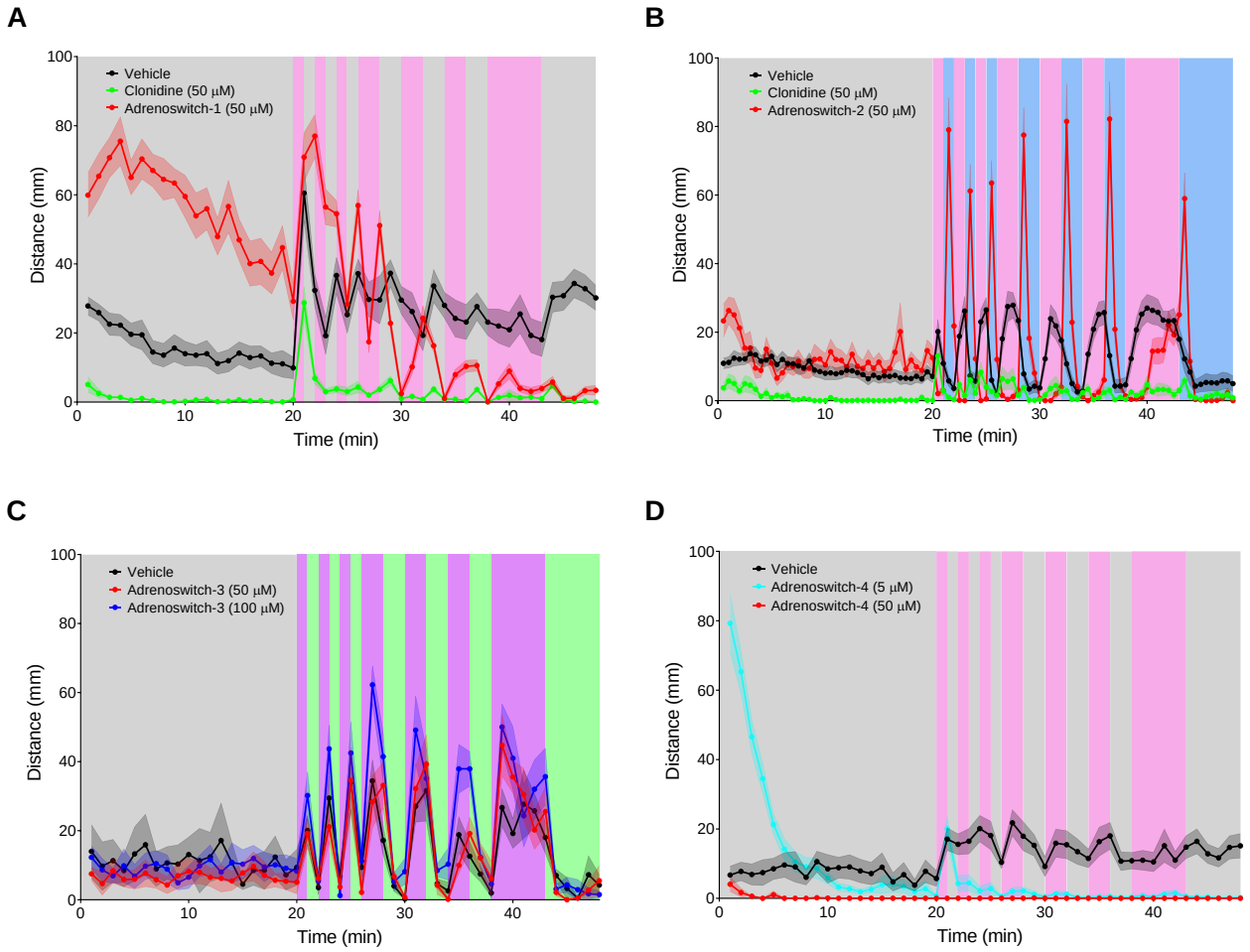

Figure S9. *Danio rerio* 7 days post-fertilisation larvae swimming activities were analysed (movements with velocities over 6 mm·s^{-1}) in one minute bin intervals for a total of 48 minutes with light variations and different treatments: 1% DMSO (vehicle), 50 µM clonidine and indicated concentrations for adrenoswitches (see legends). For adrenoswitches -1 (**A**) and -4 (**D**), after 20 minutes of darkness (relaxation period, RP) 365 nm illumination cycles were applied (purple bars). For adrenoswitch-2 (**B**) and -3 (**C**), RP was respectively followed by 365 nm and 380 nm illumination (purple and violet bars, respectively) and by 455 nm and 500 nm illumination (blue and green bars, respectively). A total of 12 (for adrenoswitches -2 and -3) and 24 (for adrenoswitches -1 and -4) larvae were used per each treatment. Error shading area represent standard error of the mean (SEM).

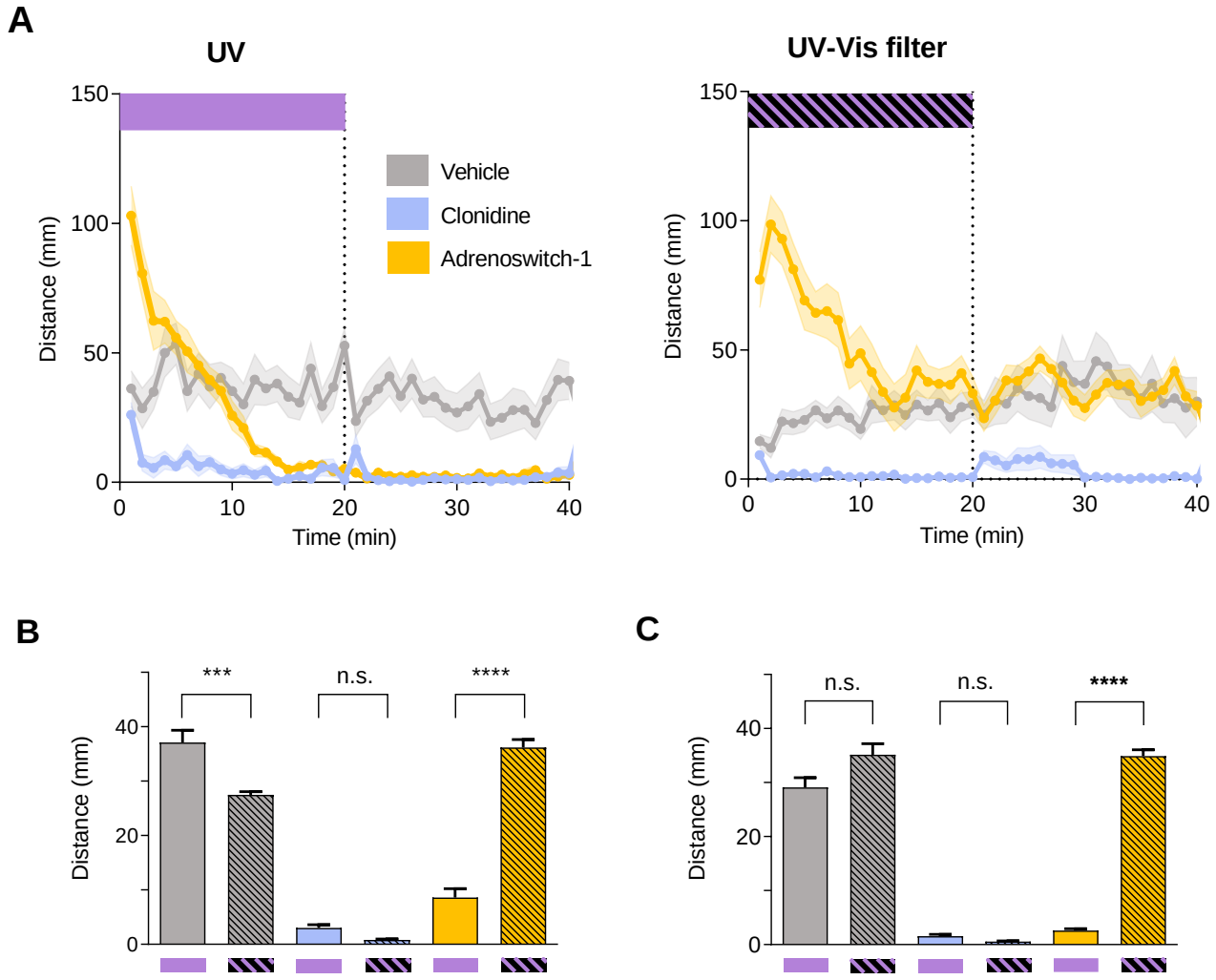

Figure S10. Time-resolved effect of adrenoswitch-1 as a function of UV light. Under UV, swimming distances are reduced to clonidine-like levels whereas in the absence of illumination (through a UV-Vis filter with a cut band over 780 nm) swimming distances are equivalent to the vehicle control. **A)** *Danio rerio* 7 days post-fertilisation larvae swimming activities were analysed (movements with velocities over 6 mm·s^{-1}) in one minute bin intervals for a total of 40 minutes (20 minutes with UV illumination followed by 20 minutes of darkness) and different treatments: 1% DMSO (vehicle), 50 µM clonidine and 50 µM adrenoswitch-1 (left panel, see legends). Each treatment was simultaneously duplicated under a UV-Vis filter with a cut band over 780 nm wavelength (right panel). A total of 12 larvae were used per each treatment. Error shading area represent standard error of the mean (SEM). **B, C)** Quantification of the swimming activity shown in **A)** under different illumination and drug exposure during the time intervals 10-20 min (**B**) and 30-40 min (**C**). Data represent means ± SEM. Statistical differences between UV- and non-UV-exposed larvae were determined by two-way ANOVA with Tukey's multiple comparison test (n.s.; not significant; ***, *p*-value ≤ 0.001; ****, *p*-value ≤ 0.0001)

In vivo pupillometry in blind mice

Opn4xRd10 mice

Experiments of pupillary light sensitivity and photometry were performed using completely blind mice which lacked both cones and rods and presented dysfunctional melanopsin cells. All individuals shared the same genetic background (C57BL/6J strain). Blind mice are the result of backcrossing between *Rd10* and *Opn4-/-* animals[3,4]. When two-months-old, these animals have suffered a degeneration of cones and rods therefore they have no photopic or scotopic vision and do not express melanopsin in ipRGC cells. This means they lack circadian synchronization and activation of the retinohypothalamic pathway.

Pupillometry

Animals were maintained anesthetized during the whole procedure using isoflurane gas (Isoflo©, ECUPHAR). Anaesthesia was induced using an isoflurane vaporiser TEC 3 (MSS) and maintained with a constant gas flow of 1.5 % volumes of isoflurane at 0.6 L/min of O_2. In order to keep their body temperature constant, mice were place onto a closed-circuit thermal mat (T/Pump TPP522, Gaymar Industries) set at 37˚C.

Following a 5-minute stabilization period under dark-adapted conditions, 5 µL of vehicle (1% DMSO in PBS, pH = 7.4) were topically administered to the right eye of the animal. The pupil was allowed to stabilize for a further 5 minutes before being exposed to 8 minutes of UV light (380 nm) followed by 8 minutes of darkness. During this observation period no significant changes in pupil size were observed as a consequence of topical vehicle administration. Exposure to UV light did not evoke any pupillary responses either, confirming blindness of the animals. Subsequently, the drop of residual vehicle was carefully cleaned from the eye before applying 5 µL of a 1 mM solution of adrenoswitch-1 (0.02% w/v). The pupil was again let stabilize in the dark for 5 minutes, before being exposed to intervals of UV light and darkness of 8 minute each. The robustness of the photoregulation was probed with at least two full cycles of alternating UV light and darkness intervals. Mydriasis was observed in 50-60% of the sample. At the end of the experiment, the animal was left to recover on a thermal blanket in a cage containing sawdust. Recovery generally occurred in a few minutes after the mouse had been removed from the isoflurane/O_2 mixture.

An infrared camera (Golmar, Barcelona, ES) coupled to a fixed focus microscope (Wild Heerbrugg, Gais, CH) with the focal point set at 15 cm from the lens was used to assess pupillary responses. Photos of the eye were acquired every 10 seconds from the moment anaesthesia was induced in the animal until all the light cycles had been performed.

Data analysis and statistics

Pupil areas were measured using the Fiji (ImageJ) software. Data were analysed and processed using GraphPad Prism v8.3.1 Statistical differences between two means were determined by Student' *t* test for unpaired observations. *P* values less than 0.05 were considered to indicate statistically significant differences.

Additional references

1. Ray, U. S., Mostafa, G., Lu, T. H. & Sinha, C. Hydrogen bonded perrhenate-azoimidazoles. *Cryst. Eng.* **5**, 95–104 (2002).

2. Khalifa, M. E., Abdel-Latif, E. & Gobouri, A. A. Disperse Dyes Based on 5-Arylazo-thiazol-2-ylcarbamoyl-thiophenes: Synthesis, Antimicrobial Activity and Their Application on Polyester. *J. Heterocycl. Chem.* **52**, 674–680 (2014).

3. Chang, B. *et al.* Two mouse retinal degenerations caused by missense mutations in the β-subunit of rod cGMP phosphodiesterase gene. *Vision Res.* **47**, 624–633 (2007).

4. Peirson, S. N. *et al.* Expression of the candidate circadian photopigment melanopsin (Opn4) in the mouse retinal pigment epithelium. *Mol. Brain Res.* **123**, 132–135 (2004).